Received: 8 September 2023 | Revised: 22 October 2024 | Accepted: 23 October 2024

DOI: 10.1002/esp.6025

RESEARCH ARTICLE

ESPL WILEY

Morphological and fish mesohabitat dynamics following an experimental flood under different sediment availability

Tulio Soto Parra[1] | Emilio Politti[1,2] | Guido Zolezzi[1]

[1]Department of Civil, Environmental and Mechanical Engineering, University of Trento, Trento, Italy

[2]Water Security Research Group, International Institute for Applied Systems Analysis, Laxenburg, Austria

Correspondence
Tulio Soto Parra, Department of Civil, Environmental and Mechanical Engineering, University of Trento Via Mesiano 77, 38123, Trento, Italy.
Email: tsotop@gmail.com; tulio.soto@unitn.it

Abstract

Experimental floods have been increasingly used as a promising practice to rehabilitate river ecosystems downstream of dams; however, the morphological and habitat dynamics they determine under different sediment supply conditions still poses relevant research and management questions. This study investigates the morphological and fish mesohabitat dynamics following an experimental flood, in two river reaches subject to different sediment supply regimes. We chose the lower Spöl River (Switzerland) as a relevant case study, subject to an experimental flood program for several years. Downstream of the dam, a tributary supplies large amounts of sediment to the Spöl dividing the study area into two homogeneous reaches with different sediment availability but similar flow conditions during the experimental flood. We analyzed and quantified the changes in morphology and fish habitat suitability for the Brown Trout (*Salmo trutta*) at the mesoscale in these two reaches caused by the 2021 experimental flood, which lasted 11 h and had a peak magnitude corresponding to a 1-year return interval in the pre-dam flow regime. We found almost no correlation between changes in the channel morphology and in habitat suitability for this event. In the upstream reach, located immediately downstream of the dam, we observed a narrower channel with a regular longitudinal sequence featuring nearly immobile coarse rapids, interspersed with more dynamic, finer riffles. Here, reach-scale morphodynamics and the shifts of the mesohabitat mosaic and the suitable habitats were below 10%. Conversely, the downstream reach, characterised by a wider channel and much higher sediment supply of well-sorted, finer bed material, was dominated by alternate bar instability and migration at the reach scale, which caused a 45% shift in its pre-flood habitat mosaic. Nevertheless, in the same reach, the overall suitability of habitats remained relatively unchanged. We attributed these different dynamics to two main factors: (i) more prolonged bedload mobility conditions and (ii) the occurrence of bar migration in the downstream reach compared to the upstream one. This study (i) underscores the critical importance of considering sediment supply from downstream tributaries when designing and monitoring the effects of experimental floods, (ii) supports the use of morphodynamic models in the related planning and monitoring phases and (iii) shows the relevance of integrating morphodynamics and eco-hydraulic analysis to support the implementation of such flow restoration programs.

KEYWORDS
artificial floods, ecological floods, eco-geomorphic flows, fish habitat, morphodynamics, sediment supply

1 | INTRODUCTION

Flow regulation from dams has greatly changed rivers' natural flow and sediment supply regimes, causing adverse impacts on the water quality, physical habitat and biological components (Richter et al., 1996; Poff et al., 1997), often leading to ecosystem degradation, habitat loss, and homogenization (Brandt, 2000; Williams & Wolman, 1984). Simultaneously, dams provide multiple benefits to human societies in terms of hydropower production, water supply for irrigation, and multiple other uses (Bundi, 2010; Ellis & Jones, 2013; Graf, 2006). This creates a well-known environmental dilemma requiring new dam management and operational strategies.

In the last decades, setting ecological flows (or 'e-flows') has been employed in many countries around the world as a viable strategy to counterbalance the effects of river regulation (King & Louw, 1998; Kennard et al., 2010; European Commission & Directorate-General for Environment, 2015). E-flows initially consisted of establishing a constant minimum flow aiming at limiting extreme negative ecological impacts on downstream river ecosystems, with a particular focus on fish. However, further research has demonstrated that these constant flows, computed from purely hydrological approaches based on the analysis of flow time series, could not properly address the desired ecosystem functions and offered only minimal mitigation of the impacts caused by river regulation (Jalón et al., 2017; Poff & Matthews, 2013). Several researchers (e.g., Bovee, 1982; Capra et al., 1995) have pointed out that methods for setting ecological flows should focus on restoring physical processes that are actually felt by the biota. This has spurred the adoption of eco-hydraulic approaches for e-flows, such as the assessment of river habitat integrity (Parasiewicz, 2007; Schneider et al., 2010).

Habitat modelling has become widely used by scientists and river managers to design and assess the effects of e-flows and flow restoration scenarios (e.g., Dunbar et al., 2012; Suska & Parasiewicz, 2020; Vezza et al., 2014; Vassoney et al., 2019). Most habitat models assume a static river morphology and predict that habitat variability in time is only due to flow variability. Yet, considerable adjustments in habitat availability for a given channel morphology can occur after floods, river restoration projects, and dam removals, suggesting the central role played by sediment supply too (Bundi, 2010; Lane et al., 2020; Poff et al., 1997; Rachelly et al., 2021; Whipple & Viers, 2019). A paradigm shift is needed from what can be called "fixed-bed habitat modeling" to "mobile-bed habitat modeling". This can be associated with the recent recognition of the analogous importance of the "natural sediment regime" (Wohl *et al.* 2015) in tandem with the "natural flow regime" paradigms (Poff et al., 1997) for the functioning of riverine ecosystems.

Changes in water and sediment availability have significant impacts on river morphodynamics across a range of spatial scales, from reach-scale to micro-scales (Schumm, 1977; Surian, 1999; Scheurer & Molinari, 2003; Thorne et al., 1997). Reduction of flood frequency and sediment supply because of dams can result in alterations to the river structure, including channel narrowing, channel incision, and a decrease in braiding intensity (Surian & Cisotto, 2007), ultimately leading to habitat loss. Aquatic habitats are heavily affected by processes of morphological change, which are dependent on the transport capacity and sediment supply of the stream, and also on the sediment size distribution. For example, excessive deposition and a lack of erosion can cause colmation, therefore reducing spawning areas for fish and leading to declines in egg and early life stage success (Ingendahl, 2001; Greig et al., 2007; Wildhaber et al., 2014).

Advances in approaches to partially restore the natural sediment regime have emerged over the last decades, including experimental floods, which encompass intentional releases of water from dams or reservoirs, aimed for diverse purposes such as sediment transport management, reservoir maintenance, ecological restoration, and habitat enhancement downstream of dams (Acreman, 2000). As the quantification of the short- and long-term effects of these floods still pose numerous challenges, these floods are often managed as experimental measures (Robinson et al., 2003; Robinson et al., 2023). Other measures, where feasible, are sediment bypass tunnels, designed to redirect and transport sediment around the dam, preventing it from accumulating in the reservoir and thereby preserving the dam's operational efficiency and longevity, while partially restoring sediment connectivity downstream (Boes et al., 2014). Experimental floods are part of the broader class of managed floods and have demonstrated efficacy at improving ecological conditions downstream of dams and reservoirs in a timespan of decades (Robinson et al., 2003; Robinson et al., 2018). Experimental floods are often meant to restore and preserve ecological functions, and resources and are planned in collaboration with local stakeholders (Acreman, 2000). While they have been proven effective for restoring wetlands and floodplain habitats, enhancing fish population recovery and increasing macro-invertebrate density (e.g., Acreman, 2000; Doering et al., 2021; Ortlepp & Mürle, 2003; Poff, 2002; Robinson et al., 2003; Sommer et al., 2001; Terrado et al., 2014; Talbot et al., 2018), quantitative assessments of their effects on the river morphodynamics and the instream fish habitat suitability and turnover are however mostly lacking at present. A recent work by van Rooijen et al. (2022) observed significant morphological alterations following a natural flood in the Moesa River, Switzerland. Nonetheless, fish habitat suitability remained unchanged despite the morphological changes. Also, the role of different sediment supply regimes on fish habitat variability in space and time has seldom been quantitatively assessed.

In this study, we aim to contribute to a quantitative understanding of both river morphological dynamics and the linked mesoscale habitat dynamics following an experimental flood event under different sediment supply conditions. To this aim, we investigate and relate morphological change (at the reach scale) and habitat shift (at the subreach scale) occurring on two contiguous reaches of the gravel-bed Spöl River (Switzerland) subject to the same experimental flood from an upstream dam. The two reaches are separated by an unregulated lateral tributary that supplies very high (though unquantified) rates of gravel as bedload to the Spöl River, thus determining very different sediment supply availability but similar flow conditions between the two reaches during the experimental flood.

2 | STUDY SITE

The Spöl River catchment encompasses an area of 286 km^2 and is located in the central Alps, spanning across Italy and Switzerland. The largest portion of this catchment is shared between the Stelvio National Park in Italy and the Swiss National Park (SNP). The Spöl River ultimately merges with the River Inn near Zernez, Switzerland,

which subsequently contributes its waters to the Danube (see Figure 1).

In 1956, a cooperation project between Italy and Switzerland to produce hydropower electricity from the Spöl waters was approved. Between 1960 and 1969, two major structures were built on the lower Spöl River: the dam at Punt dal Gall (164 Mm^3 reservoir volume capacity) and the dam at Ova Spin (6.2 Mm^3 reservoir capacity Scheurer & Molinari, 2003). In this area, the Spöl flows through a V-shaped gorge, confining it into a narrow valley. Our study sites are located downstream of the Ova Spin reservoir, near and within the SNP, where the river initially flows through a deep, rocky gorge with no relevant tributaries but some ephemeral springs, until its confluence with the Ova da Cluozza tributary (referred to as "Cluozza River" in the following). The Cluozza River catchment covers an area of 26.9 km^2, mostly northward facing, with an annual average precipitation of 887 mm. Its flow regime is predominantly influenced by the seasonality of snowmelt. During winter months, low flows typically range between 0.2 and 0.8 m^3/s, while summers can be characterized by floods with peaks up to 8 m^3/s (Consoli *et al.*, 2022; von Freyberg et al., 2018). Most of the Cluozza River flows into a confined valley with steep slopes, with a mean topographic gradient of 0.59. A hydrometric gauging station is situated at the mouth of the river where it enters the Spöl (see Figure 1c), providing real-time, publicly available flow data since 1962 (Swiss Federal Office for the Environment-FOEN). A secondary, minor ungauged tributary, the Ova da Laschadura, with a catchment area of 8.26 km^2, joins the Spöl approximately 2 km downstream of the Ova Spin dam. Its catchment area is roughly one-third the area of the Cluozza catchment; it has a prevalent southward exposure and lower highest elevations compared to the Cluozza. During snowmelt, its flow contributions to the Spol can be considered negligible, as also supported by visual observations during the release of the experimental flood. Consequently, its contribution has been neglected from the rest of the analysis.

The Cluozza River is of great importance because it allows small natural high flows to occur (see example in Figure S1) and especially because it carries, though not quantified, large amounts of sediments into the lower Spöl (Consoli *et al.*, 2022; Ruiz-Villanueva et al., 2022; Scheurer & Molinari, 2003). This produces, within the same segment of the Spöl River, two reaches with markedly different sediment availability, making for an interesting case to investigate the role of different sediment supply in channel morphological dynamics and the related habitat shift and suitability. Our analysis focused on both reach-scale and geomorphic unit-scale morphodynamics and habitat shift. To this aim, we selected two representative subreaches within the larger reaches: an upstream subreach located 500 m upstream of the confluence with the Cluozza River, within the SNP, and a downstream subreach located about 1.5 km downstream from the confluence, near the town of Zernez (Figure 1).

The upstream river reach, located between the dam and the confluence, stretches approximately 3 km and flows through a gorge. It showcases the characteristics of a typical confined mountain stream, featuring rapids and riffles, with boulders, steep slopes, and a limited floodplain area. The downstream reach spans from the confluence with the Cluozza River down to the Inn River, for roughly 2.5 km, is partially confined by bank protection structures and passes through the village of Zernez with gentler slopes and a larger floodplain. Already at

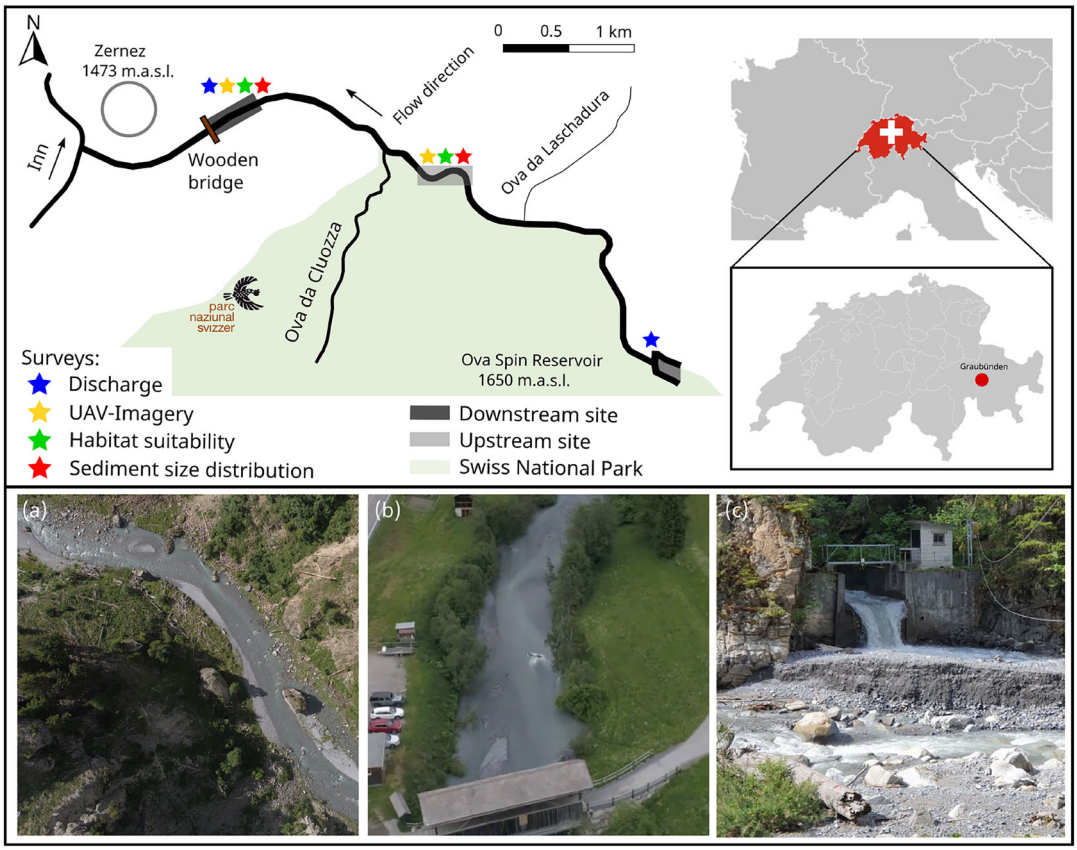

FIGURE 1 Upper panel: Map of the study area with study sites and location of the realized surveys, Swiss National Park, Switzerland. Lower panel: Views of (a) the upstream reach, (b) the downstream reach, and (c) the confluence with Ova Cluozza lateral tributary.

moderate-high flows, this river section undergoes visible morphological changes. In this reach, the upper segment, from the confluence for approximately 1.2 km, the channel is partially confined, featuring vegetated islands and a meandering form. Within this segment, woody debris is notably abundant, primarily sourced by vegetated side valley slopes (Pellegrini et al., 2022; Ruiz-Villanueva et al., 2022). On the other hand, the lower segment, encompassing our study subreach, extends for roughly 1.3 km and exhibits a braided morphology characterized by alternating bars and expansive floodplains.

Since 1996, an agreement among the Swiss Cantonal federal government, the power company Engadiner Kraftwerke AG and the SNP promoted the release of yearly experimental floods aimed at improving Spöl's ecological conditions (Scheurer & Molinari, 2003). The main objective was to improve the riverbed and habitat conditions for a variety of species including the native Brown Trout (*Salmo trutta fario L.*), which had been negatively modified by the flow regulation imposed by dam operations since 1970 (Scheurer & Molinari, 2003). The experimental character of the ecological floods program is aimed at understanding and setting flood characteristics consistent with the achievement of set environmental targets (Mannes et al., 2008; Robinson et al., 2017; Robinson et al., 2018). After the approval of the program, in January 2000, floods have been released from both Punt dal Gall and Ova Spin dams into the Spöl since the year 2000. The release of ecological floods from the upper Punt dal Gall dam into the middle Spöl has had a positive impact on the macroinvertebrates community and fish habitat, bringing them closer to the conditions expected in an Alpine River like the Spöl (Mannes et al., 2008). However, the percolation of pollutants from the dam caused an interruption of the flood program in this river segment in 2016. The floods from the Ova Spin Dam have been implemented uninterruptedly since the year 2000, with only a couple of exceptions due to unfavourable hydrological conditions that would have adversely affected hydropower production. The periodic release of these floods over the years eroded debris fans and transported sediment downstream (Ortlepp & Mürle, 2003).

3 | MATERIALS AND METHODS

Our study integrates field data collection, simplified sediment transport capacity and theoretical morphodynamic modeling, analysis of aerial images and mesoscale habitat suitability modeling to assess how the river morphology and the associated habitat suitability changed in response to an experimental flood in the two distinct reaches. These reaches have a very different sediment availability because of the lateral sediment input from the Cluozza River tributary. However, they experienced similar flow conditions during the experimental flood, as the average flow contributions from the Cluozza represent only a small fraction (<10%) of the peak flow during the flood. The analysis has been performed in relation to the experimental flood released in June 2021, with surveys conducted before, during and after the event.

3.1 | Flow data and UAV-imagery

The designed flood magnitude was based on a 1-year return period flood in the pre-dam flow regime, with a peak discharge of 25 m^3/s. The flood lasted approximately 11 h, and the flow release was increased gradually, every 30 to 60 min, until reaching the peak discharge after about 5 h.

Since the river reach between the dam and the confluence with Cluozza River does not receive relevant water contributions, the released flood hydrograph at the dam provided by the power company was used for hydraulic and morphodynamic computations related to the upstream reach. In the downstream reach, we measured discharge continuously during the flood to account for the additional input from the Cluozza tributary and for further modifications of the flood wave associated with its propagation dynamics in the 4.6 km-long channel. To this purpose, a cross-section located 1.5 km downstream of the confluence was established slightly downstream a wooden bridge, with fixed riverbanks and without any pier in the river channel.

For the low flows, occurring the day before and after the flood, we used a handheld-magnetic-inductive meter (OTT MF Pro) to measure flow velocity and water depth at every 0.5 m in that cross-section, from bank to bank. To measure discharge during the flood, surface flow velocity was measured once every hour from the wooden bridge with a hand-held surface velocity radar (SVR, from the brand Decatur). Streamflow was then computed by integrating the SVR surface velocity measurements within the velocity-area method (Herschy, 1993; Welber et al., 2016). Specifically, we coupled bathymetry data measured at low flow conditions with continuous water level readings that were taken every 15 min from a graduated rod that we installed on the right bank of the same cross-section before the flood. We assumed a standard value of the velocity coefficient ($\alpha = 0.85$) to convert surface velocities into depth-averaged velocities. We then computed discharge every 15 min by interpolating velocity measurements performed every hour. A literature-based uncertainty value of 10% is assumed after Welber et al. (2016), which takes into consideration (a) errors associated with the choice of the velocity coefficient, (b) errors due to the limited transverse resolution of velocity profiles, (c) uncertainties in the representation of the bathymetrical profile before and after the flood and (d) systematic errors after calibration of the SVR instrument. It is indeed important to consider that even when the section under the bridge is embanked, changes in bathymetry can still occur during the flood. Though they could not be directly taken into account in this investigation, these changes likely play a minor role in discharge estimates at high flow conditions. The water level-discharge rating curve is then integrated with continuous water level readings to obtain the flood hydrograph at the downstream section.

High-resolution orthophotos from UAV-based photogrammetry were provided by the research team of the SNP. Two UAV flights were performed before and after the ecological flood over both our study reaches under similar, low flow conditions. The orthomosaics with a 1.2 cm^2 resolution were used to assess and quantify the aerial morphological changes occurred in both reaches after the experimental flood, in terms of wet and dry area distributions, which were mapped through manual digitization or delineation using a GIS platform.

3.2 | Hydromorphology and mesoscale habitat assessment

To quantify changes in the reaches' hydromorphology and habitat suitability at the mesoscale, we applied the MesoHABSIM

methodology (Parasiewicz, 2007; Vezza et al., 2014). MesoHABSIM is based on a combination of data collection strategies and analytical techniques to determine the amount of physical habitat available for a selected target biological species under specific environmental conditions (Parasiewicz, 2014). It defines suitable mesoscale units as areas where fish are likely to be observed for a significant portion of their diurnal routine, which reflects their ecological significance (Kemp et al., 1999). From a geomorphological viewpoint, mesoscale units or mesohabitats are equivalent to hydromorphological units (HMUs) in the wet river channel, also known as Geomorphic units (Belletti et al., 2017). The environmental characteristics of each mesohabitat determine their suitability, and they are described based on several habitat attributes: flow velocity and water depth distributions, substrate type distribution (including various sizes of fine sediments, gravel, and cobbles), presence/absence of cover and refugia (e.g., boulders, emerged and submerged vegetation, woody debris, Bovee et al., 1998; Kemp et al., 1999; Parasiewicz, 2014), see also Table S1). To map the HMUs in the two reaches, we followed the MesoHABSIM methodology in its standardized version for the WFD 2000/60 application at a national level in Italy (Vezza et al., 2017). We used a laser rangefinder (TruPulse 360R) and the ArcPad software to survey the HMUs polygons. Each HMU was then sampled for the distribution of substrate class, water depth, and mean flow velocity in a minimum of 10 points, where the spatial distribution of the points follows a stratified random approach. Mean flow velocity (measured at 40% of the depth from the bottom of the channel) and water depth were measured using the OTT MF Pro and an FP111 Flow Probe. Substrate class was evaluated through both visual inspection and the use of a gravelometer, whereas covers and refugia information (presence or absence) were assessed visually within each HMU.

We performed HMU mapping before and after the flood under similar discharge conditions (upstream subreach pre / post: 2.08 / 1.98 m^3/s; downstream subreach pre / post: 1.95 / 1.78 m^3/s), which were measured at the beginning of each survey, to compare the effects of the flood on the reach-scale morphology and on the mesohabitats in the two reaches. Using MesoHABSIM's SimStream-Web software (Vezza et al., 2017), we combined hydromorphological surveys with habitat preference models for the brown trout, at both juvenile and adult life stages (Vezza et al., 2012) to compute the related habitat suitability. Figures S2 and S3 show the partial dependence plots of the multivariate habitat preference models we used to compute whether each mesohabitat was optimal, suitable, or unsuitable, for both adult and juvenile brown trout. It is worth noting that the mesohabitat surveys were conducted on different days from the UAV flights. Consequently, slight differences in the distribution of wet and dry areas between habitat surveys and orthomosaic analyses can be expected.

The mesohabitat analysis was conducted on two subreaches that could be considered representative of the longer upstream and downstream reaches, based on the criteria outlined by Gurnell et al. (2016) and Rinaldi et al. (2013). A river reach can be defined as a section of the river along which driving variables (flow and sediment supply regimes) and boundary conditions (valley confinement, slope) are sufficiently uniform, and it is recognized as a suitable and meaningful spatial scale for assessing hydromorphology (Rinaldi et al., 2013). Within this context, a representative subreach refers to a portion of the reach in which the local mosaic of hydro-morphological units (HMUs; see Table S1) well represents the characteristics of the HMU mosaic of the larger reach (Belletti et al., 2017). When the reach morphology consists of repetitive morphological sequences, like alternating bars, riffle-pool or step-pool sequences, a representative subreach should then cover at least one of the fundamental repetitive units of such sequence. In single-thread river morphologies, the length of such unit typically falls within a range of 10 to 20 times the channel width (Gurnell et al., 2016; Rinaldi et al., 2013), because this is the typical spacing (or wavelength) associated with alternating bars or riffle-pool sequences (Colombini et al., 1987; Montgomery & Buffington, 1997; Zolezzi et al., 2012).

Belletti et al. (2017) and Vezza et al. (2017) also suggest that representative subreaches in single-thread morphologies should contain an HMU assemblage of at least 10 units. Based on the above criteria, for the mesohabitat surveys, we selected (i) the 300-m long subreach (~27 channel widths) highlighted in Figure S6 as representative of the upstream reach and (ii) the 120-m-long subreach (~7 channel widths) highlighted in Figure S7 as representative of the downstream reach. Though for operational reasons the downstream subreach is slightly shorter compared to the 10 channel widths, it includes roughly 20 HMUs and covers half the wavelength of one alternate bar and, therefore, one complete repetitive unit.

3.3 | Computation of sediment mobility and theoretical morphodynamics

To complement the assessment of river morphodynamics and of the shift in habitat mosaic associated with the flood, we developed two complementary approximate estimates of flow conditions for bed-load initiation at the reach scale, using (a) Barthust's method for determining a critical unit discharge for bed-load initiation, which is suitable for channels steeper than 1% (Bathurst, 1987), and (b) the classical approach based on a critical value of dimensionless Shields parameter (Shields, 1936). The critical unit discharge (Bathurst, 1987) is computed as follows:

$$q_{c-d50} = 0.15 g^{0.5} d_{50}^{0.5} S^{-1.12} \quad (1)$$

where q_{c-d50} is the critical unit discharge related to the median particle diameter (d_{50}), g is the gravitational acceleration and S is the bed slope. The reach-averaged Shields parameter (θ) has been estimated under the assumption of normal flow conditions:

$$\theta = \frac{S\,D}{\Delta d_{50}} \quad (2)$$

with D normal flow depth and Δ the sediment submerged density relative to the density of water ρ ($\Delta = (\rho_s - \rho)/\rho$). Critical Shields stress for bed-load initiation was computed after Lamb et al. (2008), as $\theta_c = 0.15 S^{0.25}$.

To assess the possible mechanisms controlling reach-scale morphodynamics and its relation with the mesohabitat shift at smaller spatial scales, we then separately computed for the two reaches the ranges of theoretical conditions for the development of migrating free bars (Colombini et al., 1987). Such analysis was based on the consideration that the development and migration of free bars is a

key mechanism promoting morphological change at the reach scale in single-thread rivers with fixed banks.

Morphological change in single-thread rivers with fixed banks, like the Spöl, mainly occurs through the migration of large-scale bedforms (bars) during floods, and through selective dissection of the same bars during the recession phase of the flood, at lower flow stages. Migrating bars in single-thread rivers are known to be 'free' bars (e.g., Colombini et al., 1987; Nelson, 1990), which develop as a fundamental bed instability process in straight or nearly straight channels (Adami et al., 2016; Miwa & Nagayoshi, 1999). Their mechanism and dynamics are somehow opposite to 'forced' bars (Blondeaux & Seminara, 1985), which originate due to external geometrical forcing (like channel curvature or spatial width variations) and do not migrate within the channel.

Linear morphodynamic theories for free bars in single-thread river channels (e.g., Colombini et al., 1987) indicate that free bars can form, or, in other words, that the riverbed is unstable with respect to free bars, only if the half-width to depth ratio $\beta = W(2D)^{-1}$ under channel forming conditions exceeds a threshold $\beta_c(\theta, d_s)$. Such threshold depends on the Shields parameter θ (Equation (2)) and on the relative roughness $d_s = d_{50}D^{-1}$. To examine how these conditions could vary within the entire involved range of bedload-transporting discharges during the experimental flood, we have computed two sets of (β, β_c) values for each reach. We estimated the reach-averaged values of the aspect ratio β and of its threshold for free bars formation β_c at the flood peak and at the discharge corresponding to the estimated entrainment threshold for the d_{95} proposed by Eaton et al. (2020) as the entrainment threshold for channel-forming processes in gravel beds, corresponding to the shear stress capable of mobilising 80% of the bed surface. The values of the threshold β_c for the upstream and downstream reaches have been computed through our own developed TREMTO (Theoretical RivEr Morphodynamics TOol) code that is based on Colombini et al. (1987).

For the computations, an estimate of the reach-averaged normal water depth for both reaches at all stages of the flood was required. For this, we extracted the channel average width and slope from the UAV-derived orthoimages and Google Earth imagery, respectively. We averaged 30 equidistant cross-sectional widths per reach. Finally, we calculated a local water depth time series for an equivalent cross-section of rectangular shape that could be considered representative of reach-averaged conditions from the available discharge time series by solving the classical Manning's formula for the flow depth D (Chow, 1959):

$$Q = V \cdot A = A\, R^{2/3}\, \sqrt{S}\, n^{-1} \quad (3)$$

where Q is discharge, $A = b \cdot D$ is the cross-sectional area, R is hydraulic radius and n is Manning's coefficient.

A summary of the reach-averaged hydro-sedimentary conditions for the study reaches is reported in Table 1. The upstream area exhibits a regular sequence of rapid-riffle units. We expect different sediment mobility conditions between these rapid and riffle units, suggesting computing the related hydraulic parameters separately. For the above computations, the reach average slope was obtained by dividing the difference in elevation between the start and end of the section by the length of the reach. Grain size parameters d_{50}, d_{16}, d_{84} and d_{95} were extracted from the grain size distribution analyses. We used Manning's coefficient of 0.05 (mountain streams—gravels, cobbles, with large boulders) for the upstream rapid section and 0.04 (mountain streams—cobbles & few boulders, Chow, 1959) for the riffle section of the upstream section and for the downstream section. The values of the parameters used for computing bed-load initiation are reported in Table 1. Figure 2 shows a detailed diagram of the workflow employed to obtain such bed-load initiation estimates.

To extract the grain size distributions, we used the pebble count method after Wolman (1954). It consists of randomly selecting and measuring with a graduated sieve a minimum of 100 surface substrate particles and developing a size distribution curve for the collected grain sample of the streambed. Three sets of 100-particle counts (moving downstream to upstream and vice versa) were conducted for both study reaches, before and after the flood, to obtain reach-scale grain size distributions. We computed bed-load initiation conditions at both reaches for the entire duration of the ecological flood by relating the computed time series of the unit discharge and of the Shields parameter with their respective estimated thresholds. Though highly approximate, this approach aimed especially to quantify the reach-averaged difference in sediment mobility between the two reaches located upstream and downstream of the confluence with the lateral tributary (Cluozza). This analysis was not aimed at obtaining a detailed, spatially variable estimate of sediment mobility, for which a 2D hydraulic model would have been needed.

The observed differences in the duration and relative magnitude of sediment mobility conditions in the two reaches were then related to the observed differences in morphological and habitat mosaic change between the two reaches.

4 | RESULTS

4.1 | Propagation of the experimental flood wave

Figure 3a shows the rating curve computed through the coupled velocity, local water level and cross-sectional topography measurements conducted before, during and after the flood (Section 2) and used for the estimation of the discharge time series at the downstream section,

TABLE 1 Summary table of design parameters and river characteristics for the computation of bed-load initiation for the upstream (rapids and riffles sections separately) and for the downstream reaches.

Section	Distance from the dam (km)	Length (m)	Average width (m)	Average slope (%)	d_{50} (mm)	d_{16} (mm)	d_{84} (mm)	d_{95} (mm)	Manning's coefficient (—)	Max. discharge (m^3/s)
Upstream (rapids)	2.75	120	7	1.9	170.03	40	470	851	0.05	25.9
Upstream (riffles)	2.75	180	10.8	1.6	45.54	18	172	652	0.04	25.9
Downstream	4.75	100	21.86	1.27	22.6	11	45	63	0.04	27

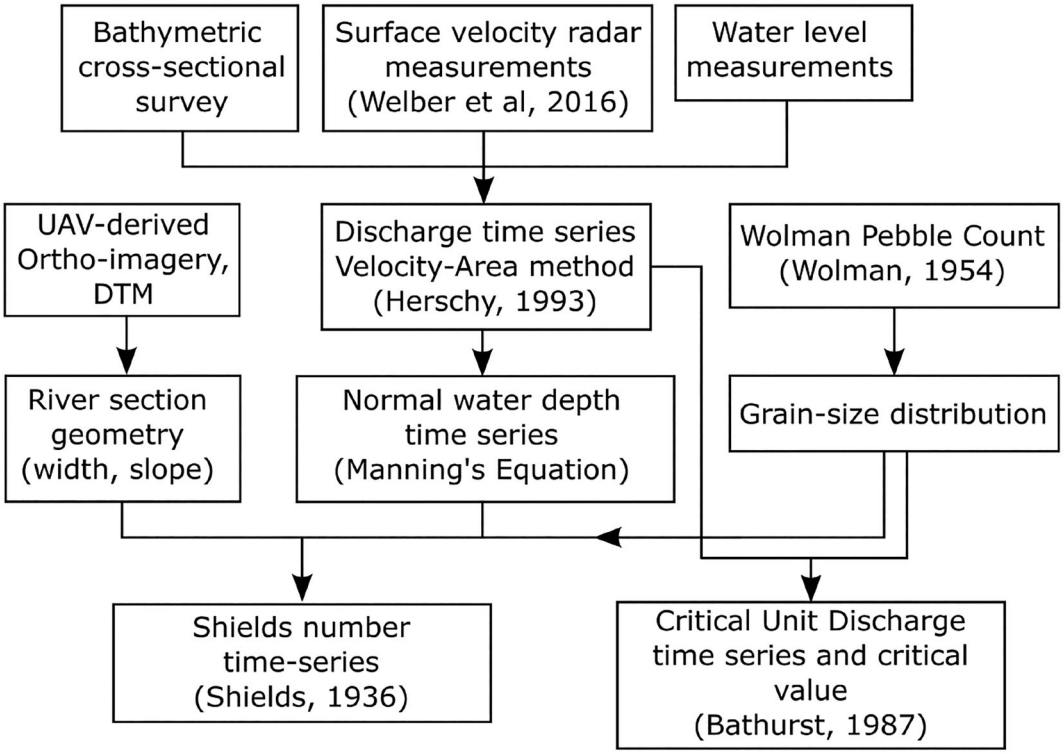

FIGURE 2 Workflow for computing bed-load initiation conditions.

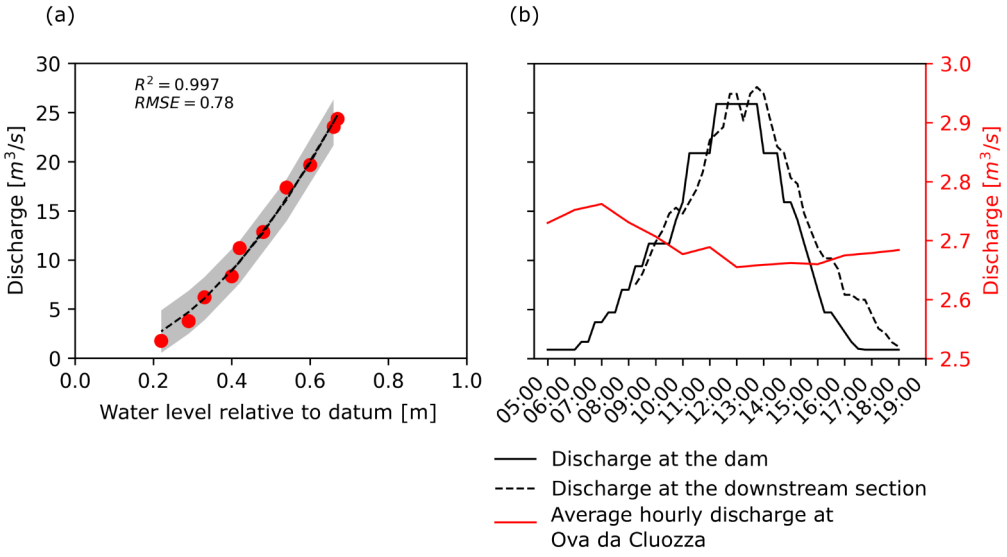

FIGURE 3 (a) SVR-derived Water Level-Discharge rating curve for the bridge downstream section; (b) Ova Spin reservoir release hydrograph, estimated discharge at the downstream section (dashed line), and average hourly discharge at Cluozza River. SVR, surface velocity radar.

reported as dashed line in Figure 3b together with the design flood hydrograph (continuous black line) just downstream the outlet from the dam. The hourly average discharge time series for the Cluozza River within the same time interval is reported as a red line.

A good agreement was observed between the measured discharge, computed with the 'standard' $\alpha = 0.85$, and an estimation obtained as the sum of the dam released hydrograph and the hourly average Cluozza River discharges (Figure S4). Such estimation provides a realistic assessment of the discharge at the wooden bridge, considering that the wave damping is highly limited by the rather steep slope (~1.6%) and the short distance traveled (~4.5 km).

Comparison between the resulting discharge wave at the downstream reach with the design hydrograph (Figure 3b) showed that the overall structure of the release hydrograph was maintained 4.5 km down to the bridge in the downstream reach, with a slight upwards shift corresponding to inflow coming from the tributary. Figure 3b suggests that the upstream and downstream reaches are subject to very similar flow conditions during the experimental flood. Cross-correlation analyses between both discharge time series showed a lag of roughly 25 min from the dam to the downstream section, resulting in an average wave celerity of 3 m/s. Such value is consistent with the estimated ranges of cross-sectionally averaged flow velocities for the discharge range between incipient bedload conditions and the flood peak, which are $1.5 \div 2.70$ m/s and $1.2 \div 2.0$ m/s for the upstream and downstream subreach, respectively. Indeed, it is well-known that the speed of the flood waves is slightly higher than the average flow velocities during the flood by a factor that commonly ranges between 1 and 2 depending on the cross-sectional morphology (Chow, 1957). The average flow of the Cluozza River (Figure 3b, red line) during the experimental flood was 2.7 m^3/s. This value

corresponds to the average difference between the measured discharge at the downstream section (Figure 3b, black dashed line) and the discharge released by the dam (Figure 3b, black line) when aligning both time series using the computed time lag.

4.2 | Reach-scale sediment mobility and morphodynamics

Pebble counts yielded the grain size distributions at both reaches before and after the flood (Figure 4). In the upstream reach, characterized by a rather regular rapid-riffle downstream sequence, we observed that small to medium-size gravel (4–32 mm) was predominant in the riffles, while coarse gravel and boulders (64–1024 mm) were dominant in the rapids. Figure 4 also shows that after the flood, the reach-averaged surface grain size distribution in both reaches was nearly unchanged, with only a minor shifting in the coarser portion of the upstream reach curve.

Estimated bed-load initiation conditions can be observed in Figure 5. In the upstream reach, specifically in the rapid sections, the estimated bedload mobility thresholds for the local D_{50} were exceeded near and during peak flow conditions for about 3 h or 30% of the flood's duration, with a maximum relative magnitude $(q_{max}-q_c)/q_c$; $(\theta_{max}-\theta_c)/\theta_c$ of 0.3 and 0.54, respectively (Figure 5a). At the mesoscale, changes in the structure and spatial distribution of rapids were not observed. In the riffle section (Figure 5b), bedload mobility thresholds were instead topped for about 7–8 h (or 70% of the flood's duration), with maximum relative magnitudes of 4.5 according to the unit discharge approach and 2.58 for the shields number approach. In the downstream reach (Figure 5c), sediment mobility thresholds were surpassed for approximately 9 h (80% of the total duration), with maximum relative magnitudes of 5 and 3.

Observations of the reach-scale morphology and the morphological changes following the flood were also clearly different between the two reaches. The upstream reach (Figure S6) is characterized by a repetitive, fairly regular downstream sequence of riffles-glides and rapids-pool assemblages. The reach-scale morphology of the upstream reach remains substantially unchanged (Figure S6). Instead, in the downstream reach (Figures 6 and S7), the bed morphology is characterized by a fairly regular bar pattern. Despite some localized irregularities, a rather clear sequence of alternate bars can be recognized both before and after the flood (Figures 6 and S7). Comparing the bar structure in terms of wet/dry channel bed areas before and after the flood at very similar flow rates (see Sections 2 and 2 for more details), most of the alternate bars appear to have migrated during the flood, as suggested by the comparisons reported in Figure 6.

Linear morphodynamic theories (Table 2) reveal a coherent pattern with the field observations above. Their application also indicates different conditions for the linear stability of free, migrating bars between the two reaches.

In the upstream reach, computations have referred only to the riffle sections because only their sediment mobility has likely occurred for a consistent proportion of the flood event (7.5 hours, 68% of the flood duration). The outcomes of the analysis are reported in Table 2. In terms of ranges of β and β_c that correspond to those input conditions and the possible uncertainties in their estimation and the assumptions adopted (namely, the closure relation used for the bedload transport capacity). It appears that necessary conditions for free bar instability (i.e., formation) have always occurred downstream, where β has exceeded β_c for the entire bedload transporting conditions, while these conditions occurred only partially in the upstream reach, where β was lower than β_c at the flood peak.

4.3 | Subreach scale morphological changes and shift of the HMU assemblage

The reach-scale morphodynamic analysis, revealing the predominant alternate bar structure of the river bed in the downstream reach,

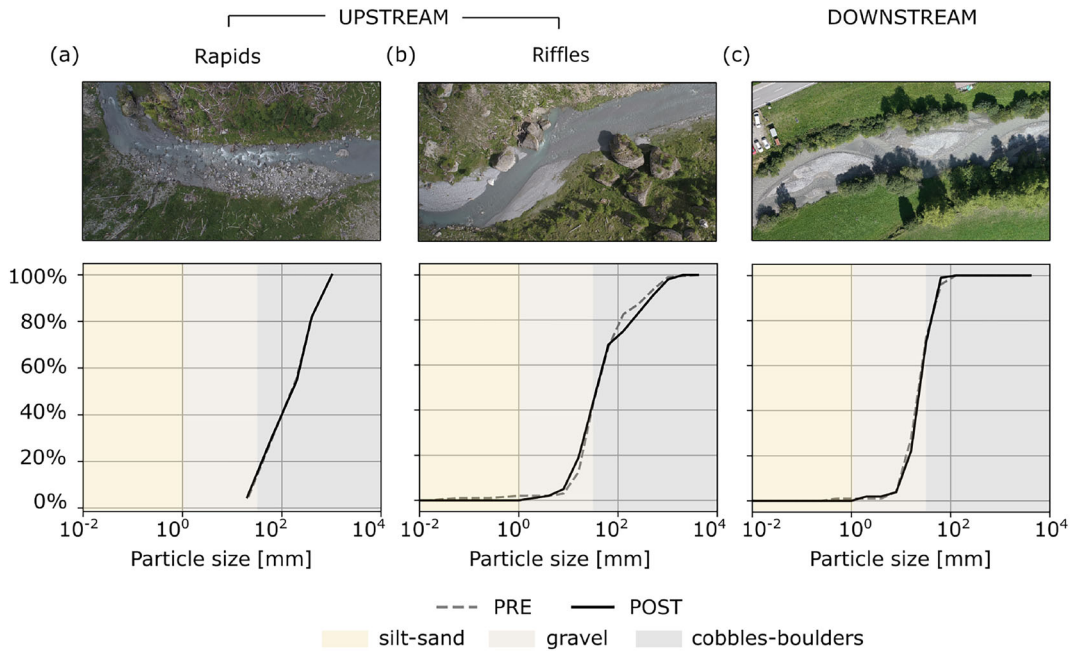

FIGURE 4 Grain size distributions from pebble counts before and after the experimental flood: (a) upstream section - rapids; (b) upstream reach–riffles; (c) downstream reach.

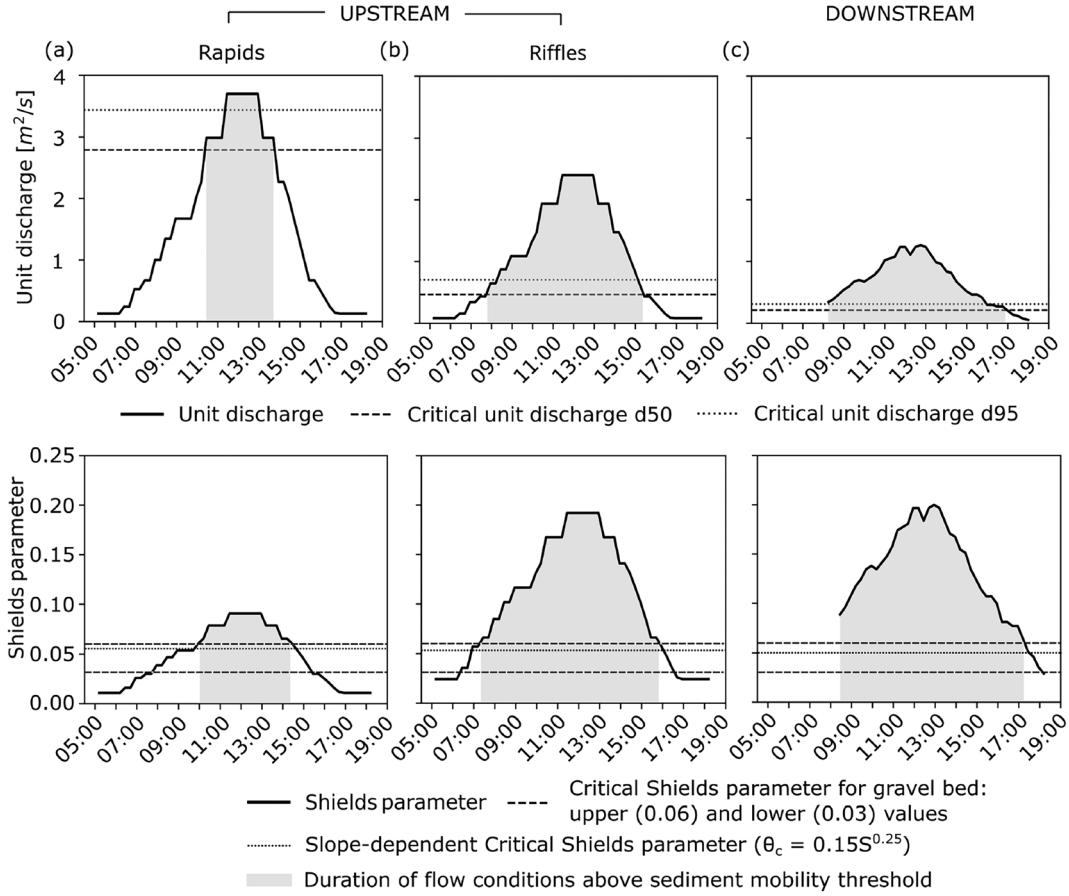

FIGURE 5 Upper panel: Calculated unit discharge time series and indication of the critical values according to Bathurst (1987) for d_{50} and d_{95}. Lower panel: Calculated Shields parameter time series for d_{50}, with the indication of the slope-dependent critical Shield parameter, computed after Lamb *et al.* (2008). (a) Upstream section—rapids; (b) upstream section—riffles; (c) downstream section.

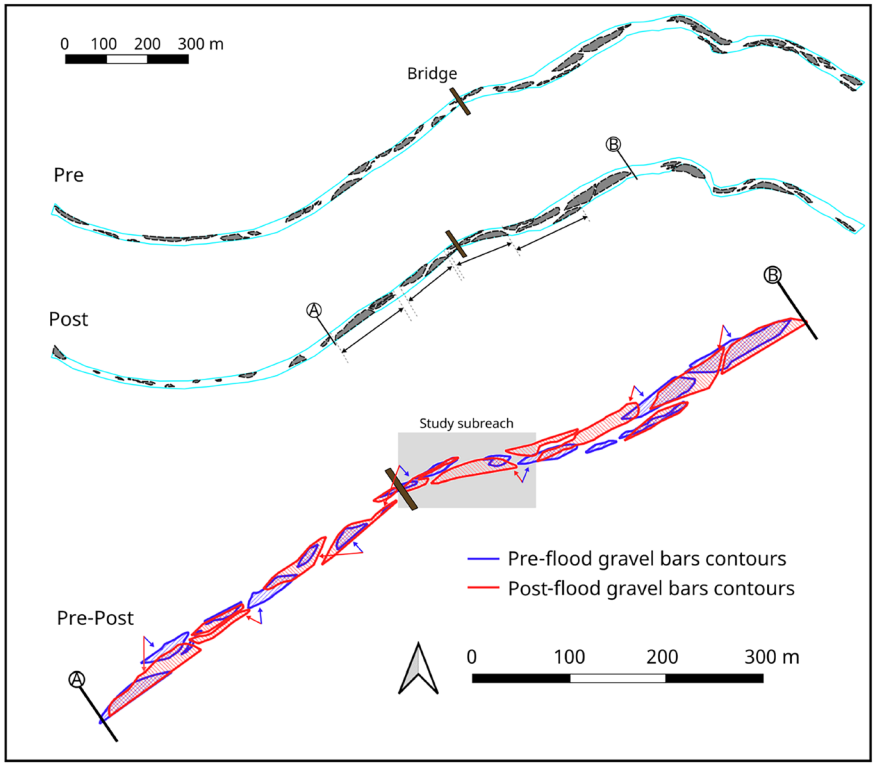

FIGURE 6 Overview of the reach-scale morphology for a portion of the downstream reach longer than the subreach in which mesohabitats have been surveyed, characterized by the presence of alternate bars which migration during the flood can be visualized in the enlarged diachronic view at the bottom. Gravel bars were manually delineated from the UAV orthomosaics. The downstream study subreach is highlighted in grey.

suggests that the selection of a subreach that is roughly as long as one length of these alternate bars can provide representative HMU assemblages for the entire downstream reach.

Figure 7 shows the morphological changes associated with the flood at the scale of the downstream subreach (reported in Figures 6 and S6). Wet and dry areas were manually delimited in the provided

TABLE 2 Ranges of theoretical conditions for free bar stability associated with the experimental flood in the two study reaches.

Linear free bars stability					
	$\theta_{d_{50}}$ range	d_s range	β range	β_c range	Free bars
Upstream reach - riffles (peak flow)	0.212 ÷ 0.318	0.033 ÷ 0.050	4.01 ÷ 4.20	6.46 ÷ 7.28	Stable (no bars)
Upstream reach - riffles (incip. bedload d_{95})	0.086 ÷ 0.130	0.081 ÷ 0.122	9.89 ÷ 10.35	4.63 ÷ 6.05	Unstable (bars possible)
Downstream reach (peak flow)	0.181 ÷ 0.271	0.028 ÷ 0.042	17.11 ÷ 17.95	6.72 ÷ 7.85	Unstable (bars possible)
Downstream reach (incip. bedload d_{95})	0.096 ÷ 0.126	0.060 ÷ 0.091	36.5 ÷ 39.1	5.03 ÷ 6.57	Unstable (bars possible)

Note: θ: Shields parameter; d_s: relative roughness; (β,β_c) aspect ratio and threshold for bar instability. Reported ranges correspond to the variability of the representative values of the D_{50}^* and of the channel slope within ±20% and ±0.001 relative to their reach-averaged values reported in Table 1, respectively, and to the use of Meyer-Peter and Müller (1948) or Parker (1990) closure relations for bedload transport.

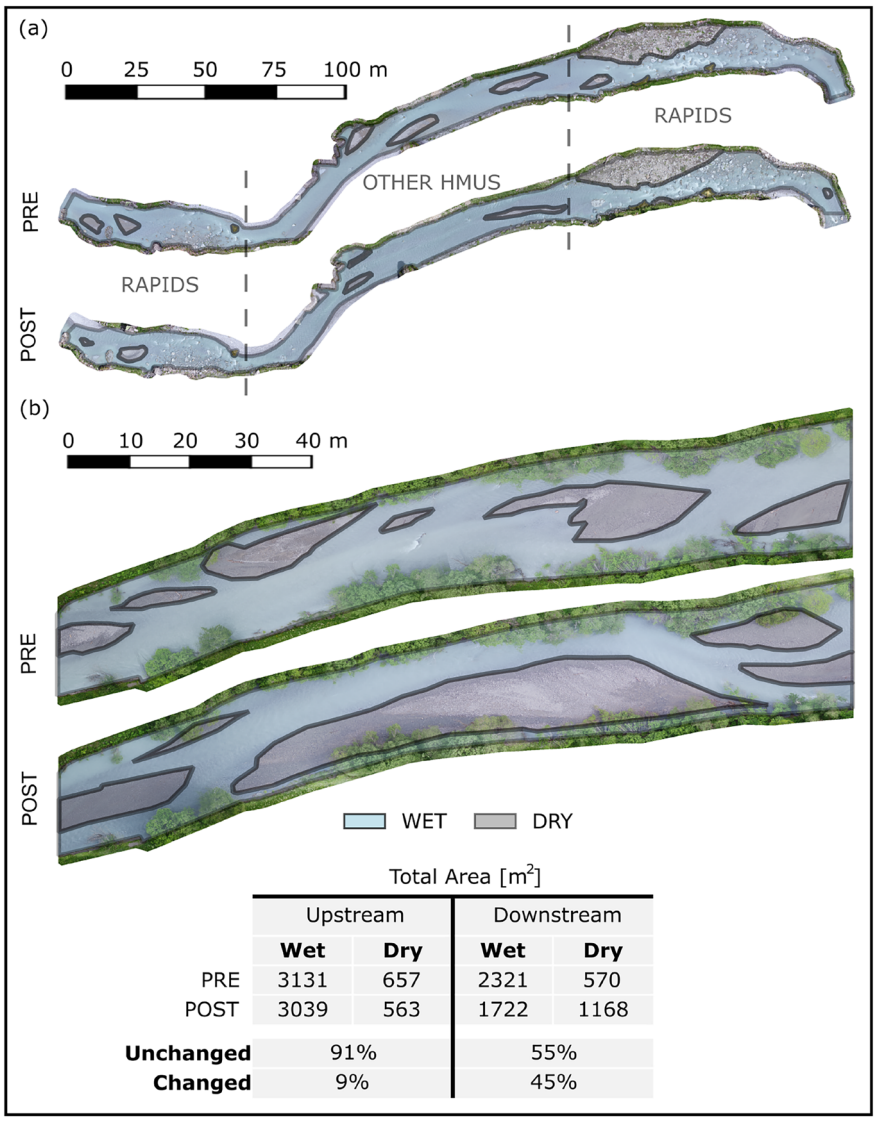

Total Area [m²]

	Upstream		Downstream	
	Wet	**Dry**	**Wet**	**Dry**
PRE	3131	657	2321	570
POST	3039	563	1722	1168
Unchanged	91%		55%	
Changed	9%		45%	

FIGURE 7 Orthoimagery delineation of wet and dry areas before and after the flood under comparable flow conditions: (a) upstream reach; (b) downstream reach.

orthomosaics resulting from the UAV surveys. The small estimated discharge difference of 0.24 m^3/s between the two UAV flights might determine slight variations in the extent of wet areas even with the same morphology. We estimated such differences to be up to 6.5% (See supporting information), therefore, with minimal effects on our results.

We spatially compared the extracted patches of wet and dry areas to quantify to which extent dry areas became part of the wet channel and vice versa (e.g., emerged bars) after the flood. Results are reported in Figure 7. Minor morphological change was observed in the upstream reach, where 91% of the total active channel area remained unchanged after the flood. The situation was considerably different in the downstream reach, in which a least 45% of the total active channel area shifted either from dry to wet or from wet to dry and, therefore, was subject to morphological change (see the small table at the bottom of Figure 7).

More in detail, in the upstream reach, only a few small emerging gravel patches in the riffle section were removed or displaced by the flood wave. The main morphological structures in the stream and the rapid sections remained fundamentally unchanged, and a slight decrease (−3%) in the total wet area could be observed. In the downstream reach, instead, the main wet channel and emerging bars

showed a general shift (Figure 6), and in the target subreach, the wet area decreased by approximately 25%, possibly due to the migration of a large side bar from upstream. Overall, this behavior is coherent with the results in Section 2, showing a much higher duration and relative intensity of bedload transport conditions in the downstream reach compared to the upstream reach, as well as with the conditions of free migrating bars instability that is predicted for the entire duration of the flood event in the downstream subreach and only for part of its duration in the upstream subreach.

Maps of the surveyed HMU mosaic for both subreaches upstream and downstream of the Cluozza River can be observed in Figure 8, before (PRE) and after the flood (POST).

The upstream reach presented a rather regular downstream sequence of shorter, steeper and coarse-substrate adjacent HMUs (mainly rapids) and longer, flatter HMUs (mostly riffles) with milder slopes (Figure 8a). This sequence repeats regularly along the entire upstream reach between the dam and the Cluozza tributary, with steeper, rapid sections being 3–9 average channel widths in length and the milder, riffle sections nearly twice as long (7–13 reach-averaged channel widths; see Figure S6). By comparing the HMU mosaic before and after the flood in the upstream reach (Figure 8a), it appears that such spatial sequence was not considerably affected by the experimental flood, with only a slight variation in the distribution of riffles (10%), although the main structure of the stream was conserved. Moreover, after the flood, we observed a decrease in the percentage area corresponding to glides (−27.7%) and rapids (−7.1%), and an increase in pool area (+25.8%), while the percentage area of riffles and dry patches varied slightly (+1.2% and +0.7%, respectively). Depth and velocity distributions in the entire reach were essentially maintained, with slightly smaller water depths and higher velocity values for pre-flood conditions. On average, HMU areas categorized by type exhibited a variation of 22.7% compared to the conditions before the flood. Notably, the predominant alterations are related to in-stream and lateral bars dynamics, which are likely controlled by the effects exerted by the major rapid structures.

Both HMU mosaics and the way they shifted spatially because of the flood were substantially different between the upstream and the downstream reaches (Figure 8b). Compared to the upstream reach, the downstream reach is overall milder in slope and is characterized by a more homogeneous bed sediment size distribution, which is

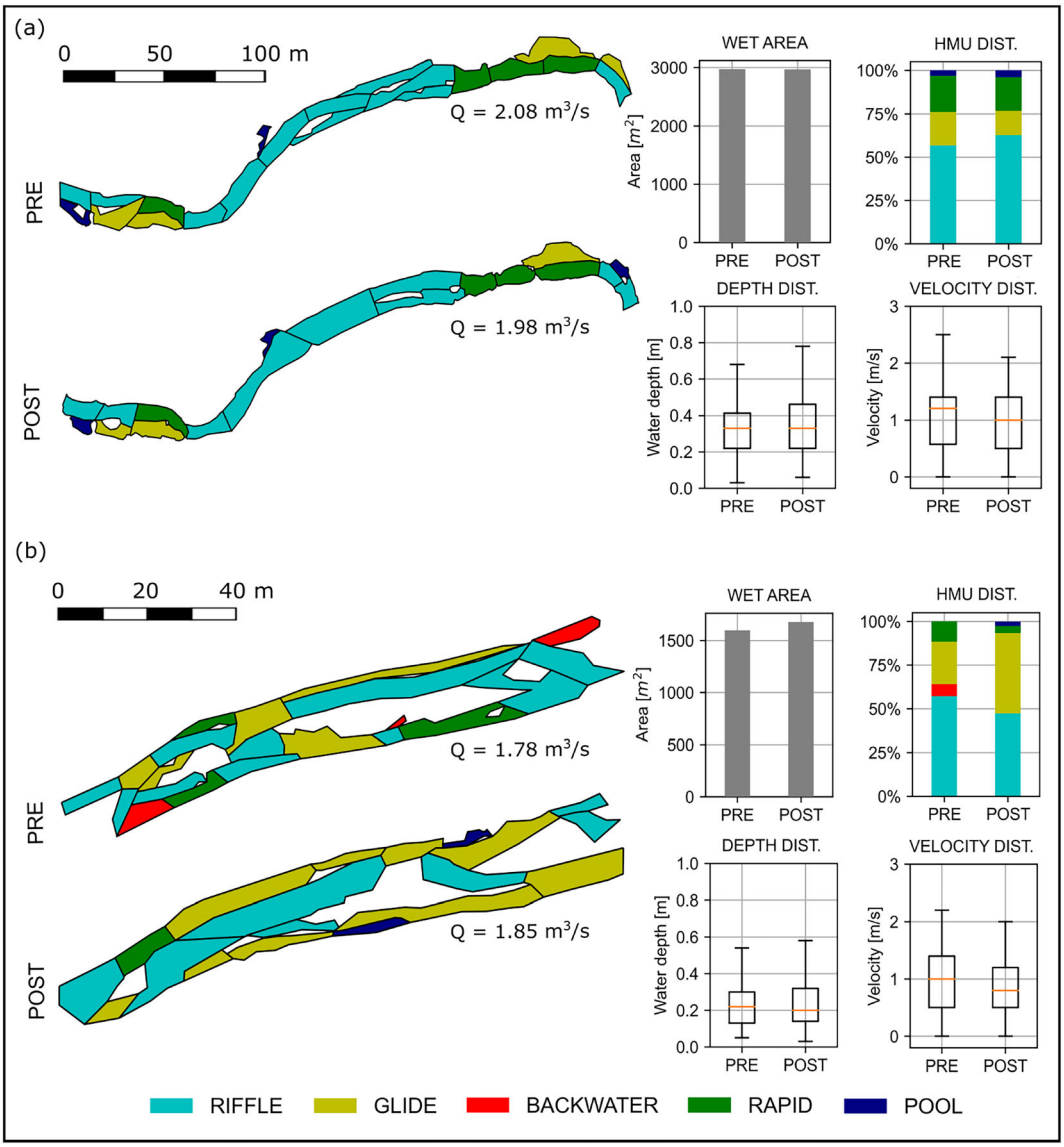

FIGURE 8 Mosaics of the hydro-morphological units (HMU), water depth and flow velocity reach-scale distributions before and after the flood: (a) upstream reach; (b) downstream reach. Q: water discharge at the time of the survey.

mainly controlled by the lateral input from the Cluozza tributary. The HMU mosaic was much more dynamic downstream than upstream. Table 3 provides the results of a spatially explicit analysis of the shifting HMU mosaic in both reaches, in terms of the altered percentage area by HMU types following the flood. Bold values highlight the percentage area of HMUs that remained the same HMU type after the flood. The dominant downstream HMUs before the flood were riffles and glides, accounting for 80% of the surveyed wet area. Despite these alterations, the depth, velocity, and substrate distribution in the surveyed reach remained relatively consistent after the flood, showing only minor variations (see left panels of Figure 8).

4.4 | Dynamics of mesohabitat suitability

Fish habitat suitability maps were developed according to the MesoHABSIM methodology (Section 2) for juvenile and adult brown trout, both pre and post-flood. Figure 9 displays the maps for adult brown trout, while Figure S5 illustrates those for juvenile trout, in both upstream and downstream subreaches. In the upstream reach, suitable habitat conditions for the juvenile trout before the flood were characterized by 17% of the total wet area being suitable and 0% optimal. After the flood, an overall decrease of about 40% of the suitable area was observed for the juvenile trout. Habitat conditions for the adult brown trout were slightly increased after the flood, from 20% to 28% of the total wet area. In the downstream subreach, suitable conditions increased for both the juvenile and adult brown trout showed a similar slight increase, overall showing little variability following the flood event. For the adult brown trout, the suitable area increased from 0 to 10% of the total wet area right after the flood.

TABLE 3 HMU spatial change matrix.

Upstream reach					
	Riffle	**Glide**	**Rapid**	**Pool**	**Dry area**
Riffle (52%)	**89.4**	0.0	0.5	0.1	9.6
Glide (17%)	9.9	**68.0**	5.9	5.9	9.9
Rapid (19%)	6.5	1.5	**90.4**	0.0	7.3
Pool (3%)	19.4	0.0	0.0	**71.3**	10.8
Dry area (9%)	11.3	6.7	1.4	7.1	**72.3**

Downstream reach						
	Riffle	**Glide**	**Rapid**	**Pool**	**Backwater**	**Dry area**
Riffle (39%)	**31.2**	39.4	1.8	0.0	1.0	25.9
Glide (16%)	28.6	**38.3**	11.0	0.0	6.0	15.3
Rapid (8%)	16.4	63.6	**0.0**	0.0	0.0	19.6
Pool (-)	Not present in preflood conditions					
Backwater (5%)	54.8	10.7	0.0	0.0	**0.0**	34.0
Dry area (32%)	40.9	13.9	0.3	0.0	3.2	**40.7**

Note: Cell values are the% area of the preflood HMU type in the row that converted into the HMU type in the column after the flood. Bold values highlight the % HMU area that remained of the same HMU type after the flood. Percentages in the first column indicate the HMU area relative to the total channel area for every reach before the flood.

Though the main focus of the present work is on the space-time habitat variability associated with the flood and not on its absolute value at the flow conditions of the surveys, it is important to explain the reasons for the relatively low habitat suitability (rearing and growth) predicted for the adult brown and juvenile trout in Figures 9 and S5, respectively. Partial dependence plots describing the probability of presence (habitat suitability) for adult brown trout and juvenile trout are presented in Figures S2 and S3, respectively. For adult fish, the probability of presence increases with combinations of water depths ranging from 0.30 to 0.60 m in at least 40% of the surveyed reach, flow velocities between 0.45 and 0.6 m/s across at least 20% of the surveyed reach, mesolithal and macrolithal substrates covering more than 20% and 30% of the surveyed reach, respectively, and notably, the presence of boulders serving as refugia. Frequency distributions of water depths, flow velocities and substrate classes surveyed pre- and post-flood in the downstream section can be found in Figure S11. Analysis of these frequency distributions reveals primarily shallow water depths within the 0- to 0.3-m range in the downstream reach. While flow velocities exhibit some variability, over 20% of values meet the preference criteria falling between 0.45 and 0.6 m/s. However, mesolithal and macrolithal substrates are sparsely present in this reach, and there is a notable absence of boulders (observed during the mapping procedure). The ensemble of these conditions motivates the rather scarce habitat suitability predicted for adult brown trout. This behaviour was also evident, especially in the riffle sections of the upstream subreach for both juvenile and adult trout (see Figure S10).

The two subreaches evidenced a different relation between their morphological dynamics and habitat dynamics (Table 4). For instance, in the upstream subreach, the changes in morphology corresponded with similar magnitudes to the habitat change. Here, the effect on habitat suitability was similar in magnitude though antagonistic for adult (+8%) and juvenile fish (−7%). In the downstream subreach, the 45% change in morphology caused by the flood was instead corresponding to only minor changes of habitat suitability for both adult (+10%) and juvenile (+1%) trout.

5 | DISCUSSION

Here, we discuss our findings to connect the reach-scale morphological changes, as observed and modelled, to the observed finer-scale dynamics in terms of the mesohabitat shift and the variations in fish habitat suitability following the experimental flood. We focus on how these dynamics differ between the two reaches, which are characterized by different channel morphology and sediment availability but very similar flow conditions, particularly during the experimental flood. We then draw some implications for the management of experimental floods and conclude by summarising the main limitations of our work and the open perspectives for future research on this topic.

5.1 | Reach-scale and HMU-scale morphodynamics and grain size distribution variability

The results of the present work show a marked difference in the morphodynamics of the two study reaches located upstream and downstream of the confluence with a high bedload-transporting tributary (Cluozza River). Nearly half (45%) of the downstream active

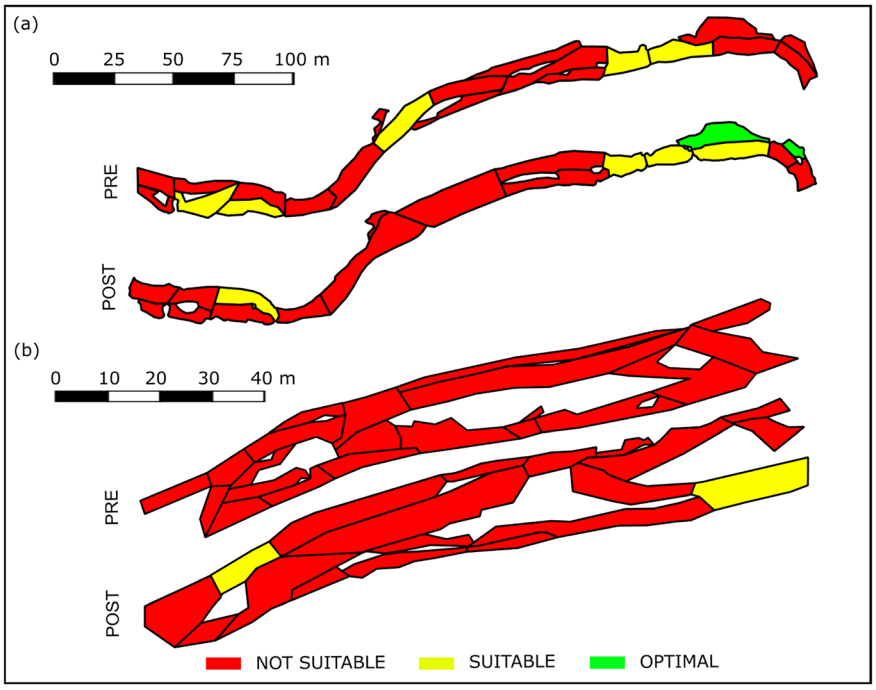

FIGURE 9 Adult Brown trout habitat suitability rearing and growth before and after the flood: (a) upstream subreach; (b) downstream subreach.

TABLE 4 Summary of morphological area change and habitat change after the flood.

Percentage of areal change		
	Upstream	**Downstream**
Morphological change	9%	45%
Adult habitat change	+8%	+10%
Juvenile habitat change	−7%	+1%

channel area showed changes in its morphology, revealed by a transition from dry to wet surfaces after the flood, while such value was less than 10% on the upstream channel area (Figure 7 and Table 3). Moreover, similar values are also obtained from the spatially explicit analysis of the changes in the different HMU after the flood (Table 3). The observed morphological change in the downstream reach is coherent with what was reported by Pellegrini et al. (2022), who observed a 76% average change in the same downstream reach after the experimental flood in September 2018, which was similar in magnitude and duration.

These upstream-downstream morphodynamic differences under basically the same flood event can be ultimately related to the difference in the sediment supply between the two reaches, which determine different bed and textural structures at two intertwined levels.

At a first level, the analysis of reach-averaged conditions for bedload initiation (Figure 5) indicates that the two reaches strongly differ for the duration of bedload-transporting conditions during the flood. The upstream reach morphology is characterized by a regular, repetitive longitudinal sequence of shorter rapids and longer riffle sections (Figure S6). Rapids have a much coarser substrate (Figure 4), with limited sediment mobility during the flood, which instead occurs within riffles (Figure 5). Such spatial arrangement is not present in the downstream reach, where the HMU mosaic is more heterogeneous, with a larger presence of glides, only occasional rapids and some backwaters. Here, sediment size is much more homogeneous, mainly reflecting the texture of the high lateral input from the Cluozza River, and conditions for sediment mobility last longer than in the upstream riffle and rapids sections (9 h rather than 7–8 and 3 h, respectively, during the flood). Shorter and spatially more fragmented bedload-transporting conditions in the upstream reach likely correspond to less likelihood of change in the HMU mosaic.

On a second level, and perhaps more importantly, the analysis of the linear bar stability (Table 2) coupled with the different morphological and textural structure of the two reaches (Figures 8 and 4) suggests that the reach-scale morphodynamics of the two reaches may be of fundamentally different nature. The condition $\beta > \beta_c$ represents one of the necessary conditions for free bars instability, together with the reach being long enough (several tens of channel widths; see, e.g., Adami et al., 2016; Serlet et al., 2018) for several bar wavelengths to develop. Such conditions are met in the downstream reach, where free bars can develop and migrate during the flood, while the condition $\beta > \beta_c$ is partially met and only in the riffle sections of the upstream reach, which, however, are too short (less than 10 channel widths each, Figure S6) for a sequence of free migrating bars to develop. This is confirmed by the reach-scale analysis (Section 2) of observed morphological change in the downstream reach before and after the flood (Figures 6 and S7), which indicates that migration of large alternate bar structures has been the main morphodynamic process characterizing the downstream subreach following the flood.

In the upstream reach, instead, free bars cannot develop and, thus, migrate. Within the hierarchy of spatial scales at which river geomorphological processes occur (Brierley & Fryirs, 2013), processes at larger scales preferentially control those at smaller ones. Therefore, we deduce that the marked difference in the temporal change of the HMU mosaic between the two reaches is essentially due to reach-scale processes, consisting of free bars developing and migrating in the downstream reach and instead being absent upstream. In this sense, the presence of the nearly immobile rapids represents a key constraint to shifting the HMU mosaic within the examined type of experimental flood.

Overall, the Spöl downstream of the dam seems to be well supplied with sediments from the valley sides, even upstream of the Cluozza River. For this reason, though not having collected detailed data on possible riverbed armoring in the upstream reach, we argue that coarse armoring of the bed, often found downstream of dams (Ferrer-Boix & Hassan, 2014; Parker, 1990), may not be a relevant cause for the observed partial transport of the stream bed (Mueller & Pitlick, 2013). The Spöl is more likely in a condition similar to what was suggested by Eaton and Church (2009); with increased sediment concentration, armoring of the streambed decreases, and the grain size of the surface sediment load approaches the grain size of the bulk streambed sediment. The characteristics of the sediment size distribution found in the downstream section are such that rather lower flows that can occur within this regulated hydrological regime can still promote sediment transport. The observed variations in the spatial distribution of HMUs and wet and dry areas in the downstream reach are coherent with the presence of a more complex morphological pattern compared to the upstream section. In a recent hydro-morphodynamic modelling study focused on the same river system, Hashemi et al. (2023) estimated that a flood with a similar magnitude to the one addressed in this paper has an average bedload transport capacity of 230 m^3 in the reach downstream of the Cluozza River, throughout the entire flood event.

In streams subject to low sediment supply regimes, often occurring downstream of dams, the flow variability may have little influence on the channel geomorphology as (1) the long exposure periods to flow regulation can create quasi-steady-state morphological conditions caused by armoring and coarsening of the streambed, strongly increasing the actual threshold θ_c for sediment mobility from its theoretical value, and (2) the sediment fractions for which the few residual flow or flood pulses are competent and are supplied neither from upstream (because of the impoundment) nor from the riverbed (because of the enhanced armoring). Moreover, as observed by Rachelly et al. (2022) from laboratory experiments, in the absence of floods exceeding the bed-forming discharge (geomorphic flows), the channel geometry of a reach with low sediment supply (lower than the total channel capacity) may remain stable for extended periods. It is only during large flood events that the stabilizing forces are surpassed, leading to substantial channel transformation. Conversely, in reaches where sediment supply is high and flow variability is low, as in the downstream section of the Spöl River, the variations of the hydrological regime, promoted by an experimental ecological flood, could increase morphological diversity by boosting sediment transport and increasing textural sorting, reducing the reliance on large floods to drive continuous widening and restructuring (Rachelly et al., 2022).

Comparing pre- with post-flood grain size distributions at the reach scale (Figure 4) indicates a negligible impact of the experimental flood in both our study sites, despite causing relevant sediment mobility, especially downstream of the confluence (Figure 5). In another study in the same river, Mathers et al. (2022) documented a significant decrease in fine sediment within riffle sections and side channels after an experimental flood, both upstream and downstream of the Cluozza River. It is crucial to highlight that their investigation focused on specific habitats or river sections, whereas the grain size characterization presented in Figure 4 focuses on the entire study reaches. More details on changes in the grain size distribution at the HMU scale can be extracted from Figures S8 and S9, where we identified the units for which the location and areas mostly overlapped before and after the flood, as sampled from the MesoHABSIM methodology. Comparison of the frequency distribution of their substrate classes highlights that some differences occurred also in relation to the present experimental flood, at the HMU scale. For the upstream subreach, most of the comparable units exhibit a small shift towards coarser substrate classes. A similar coarsening can be observed at HMU scale in the downstream section, where only a limited portion of the total area could be compared, due to modifications in the spatial arrangement and size of most HMUs following the experimental flood. While the flood may, therefore, modify grain size distribution within specific habitats (like the coarsening observed by both Mathers et al., 2022 in our study), the effect at the reach scale appears to be minimal.

5.2 | Fish habitat suitability

A key focus of our analysis is on the habitat dynamics associated with the experimental flood and its relation with morphological change caused by the same event in the two reaches. A key finding is that in the downstream reach, subject to a high supply of transportable sediment by ordinary floods (like the experimental one), the observed high shift of the HMU mosaic does not correspond to a high change of suitable habitat conditions. A similar behavior was observed by van Rooijen et al. (2022) in the alpine Moesa River, Switzerland, after a natural flood. Despite the significant alterations in habitat type and distribution, there was no observed change in suitability for the target species. The upstream subreach of the Spöl shows a complementary phenomenon, whereby the little morphological change observed corresponds to a comparable small variation in suitable habitat conditions. While a generalization of these observations would require a broader set of data, referring to a wider spectrum of flood events, and, possibly, to other river types and morphologies, what we observed is that under an ordinary flood (1-year return interval), morphological change in a single-thread river with fixed banks may not correspond to a relevant change of the suitable habitat area. In the aftermath of several natural flood events in the Moesa River, Switzerland, van Rooijen et al. (2022) observed that some floods reversed the changes in habitat heterogeneity induced by previous flood events, suggesting the potential for a dynamic equilibrium from a habitat quantity perspective, which may undergo fluctuations of up to ± 30% between consecutive states (van Rooijen et al., 2022). It might be argued that such phenomenon may not occur during much larger floods with higher return intervals (i.e., larger than 10-20 years), which can cause significant changes in the reach channel width, thus completely reshaping, and not only shifting, the habitat mosaic.

Furthermore, it must be noted that habitat changes associated with the investigated experimental floods and with the strong sediment input from the lateral tributary can result from either a shift in the mesohabitat mosaic (as in the downstream reach), or from changes in the velocity, depth, and sediment distributions within each mesohabitat, also without any shift in the HMU mosaic. Analysis of the biological models (Figures S2 and S3) and the surveyed habitat attributes (Figures S10 and S11) reveals that suitable habitats are mainly present in the rapids sections of the upstream reach (Figure 9), which are the only portion of the reaches with fish refugia, mainly provided by boulders. The scarce habitat conditions in the

downstream reach can be directly related to (1) the high intakes of sediment coming from the Cluozza River coupled with the dam-regulated hydrological regime resulting in well-sorted surface textures and (2) t the lack of morphological features that could contribute to fish refugia (see the characteristics of the biological models in Figures S2 and S3. Among these features, only overhanging vegetation was found near the banks and could provide shelter during high flows. These refugia can be described as feeding and resting areas connected with some type of cover (Robison & Beschta, 1990). In high-gradient streams, these areas generally occur as velocity shelters behind physical structures such as large woody debris or driftwood, root wads, and boulders (Fausch & White, 1981; Harvey et al., 1999; Schwartz & Herricks, 2005). Except for the rapids-dominated sections, the wetted areas of our study reaches exhibited almost no in-stream vegetation, driftwood or considerable low-velocity areas that could promote refugia for fish.

During the flood, a considerable transport of driftwood could be observed, as reported in previous floods (Pellegrini et al., 2022). However, it did not contribute to the creation of in-stream features as it was either washed away or deposited onto bar surfaces that are dry at the flow conditions of our habitat survey, which are by far the longest-lasting ones in the study reach. The absence of wood in the wetted areas of our downstream site was confirmed through both aerial imagery and on-site inspections. Although the overall suitability in the downstream reach is low and remains low after the flood, one should note that while the effect of the 2021 single flood is undoubtedly negligible on the suitability, the cumulative effects of consecutive years could increase the habitat diversity and, thus, suitability in the long run.

An aspect that could not be explored in this study is the potential enhancement of habitats for spawning fish due to the unavailability of mesohabitat-scale biological models for the spawning life stage. As noted by Mathers et al. (2021), flood waves were effective in significantly removing fine sediments trapped within the hyporheic layers, essentially unclogging the riverbed. This observation aligns with findings by Ortlepp and Mürle (2003), who reported a threefold increase in the number of fish redds following three years of annual experimental floods in the upper Spöl River.

5.3 | Management implications of ecological floods

Experimental flooding has recently been considered a promising measure to counterbalance some of the adverse effects of river regulation by dams. It plays an important role in the domain of ecological flows because e-flows are most commonly conceived as referring to the low-flow regime, often neglecting the key role of floods and high-flow pulses in restoring natural-like hydrological variability.

The analysis developed in the present work contributes to the understanding of how an experimental flood can modify the HMU mosaics in two reaches with similar flow conditions but different sediment availability and confinement characteristics. More in general, it allows us to understand how the genesis and maintenance of HMUs, for example, the form-process association (*sensu* Fryirs, 2017) creating HMUs, shape a river reach. In the particular case of this 'ordinary' flood (1-year return interval in the previous, unregulated flow regime), sediment supply seems to play an important role in the spatial shift of the habitat mosaic, which was considerably higher for higher sediment availability because of both (i) the much higher mobility of the bed material and (ii) the channel hydro-morphological conditions. In the downstream reach, with much higher sediment availability, these changes corresponded to the physical instability of alternate bars, which, therefore, could generate and migrate during the flood because the downstream channel reach provides enough suitable continuous length for their instability and migration to occur and because sediment mobility conditions last long enough for observable dynamics to happen. Awareness of these mechanisms is important when designing experimental floods as 'functional flows' (Escobar-Arias & Pasternack, 2010), defined as flows capable of causing hydro-morphological dynamics able to support ecological and morphological functions. The ecological function fulfilled by a flood depends on the process at the end, for example, ordinary floods such as the one described in this work, which has also been reported as necessary to maintain units' geometry and sedimentological differences (Almeida & Rodróguez, 2012; Vetter, 2011) and trophic suitability (Death, 2008; Poff et al., 1997). Conversely, large floods capable of reworking the planform, not investigated in this work, regenerate the riparian plant communities by eroding vegetated banks and creating new barren sites for seed recruitment (Polzin & Rood, 2006).

When setting the objective and expectations of experimental floods, managers should consider the sensitivity of the interested reaches, which in turn is determined not only by the magnitude of the flood but also by the sediment supply and the capacity of the reaches to deal with such supply. Sediment supply ultimately makes a big difference between a stable channel, such as the one in the upstream reach, able to accommodate sediment fluxes without changing the spatial configuration, and the downstream reach, which responded to the flood and associated sediment flux by highly rearranging the units. Of paramount importance in an experimental floods program is also the duration of the program itself, considering the time scale needed for the desired morphodynamic processes to occur.

Besides the outcomes referred to the specific case study of the Spol, this work highlights how the application of morphodynamic models, like the linear free bar theory in this case, can aid the prediction of possible morphological changes associated with the designed flood or can support the interpretation of the related field observations. As with other model types, analytical morphodynamic models can be used as one of the planning tools for ecological flood design.

Finally, the present study remarks on the importance of understanding the actual role of unregulated lateral tributaries downstream of dams when planning ecological floods. Previous studies in the Lower Spöl have shown that the periodic disturbances generated by the Cluozza River maintain the river in a dynamic state (Consoli *et al.*, 2022; Mathers et al., 2021). In a recent study, Lane et al. (2022) revealed that in an Alpine environment, unregulated tributaries can potentially provide enough coarse sediments to counteract the reduction caused by dams. Furthermore, the capability of natural floods from such tributaries to modify river morphology should also be considered. More importantly, sediment supply should be given considerable attention, given its significant influence as a primary driver of morphological processes such as active channel widening, sediment redistribution and lateral channel-floodplain connectivity (Rachelly et al., 2022), particularly in reaches characterized by high sediment supply, such as the downstream section of the Spöl River following the confluence with the Cluozza River.

5.4 | Limitations of this study

The analysis developed in the present work is based on several simplifying assumptions and has intrinsic limitations and uncertainties. We summarise them below.

Discharge estimations from SVR measurements have an average uncertainty of 10%, and the selection of the velocity coefficient (α) plays an important role in the accuracy of discharge values. Furthermore, changes in river bathymetry in the measured section that may occur during the flood can also affect the precision of such measurements.

The analysis of sediment size distributions and their mobility is based on several simplifications. The used approach for comparing incipient sediment mobility conditions (Section 2) cannot predict the within-reach spatial heterogeneity in bedload transport capacity, which could be achieved using a 2D hydraulic model, seems consistent with the goals of this work, which focused on comparing the two study reaches in terms of durations and relative intensities of sediment transporting conditions at the reach scale and not at the local (HMU, or even hydraulic unit) scale. Other sources of uncertainty are intrinsic in this approach, and they would be present also when applying a spatially distributed, 2D hydraulic model. Particularly, the definition of a realistic value of the critical Shields parameter for incipient sediment mobility should be calibrated with direct field observations, to support a more accurate choice in the typical range ($\theta_c = 0.03 \div 0.06$). An additional limitation is the assumption of a uniform grain size, which is, however, often made also when applying 2D models. Further work should focus on addressing the varying mobility conditions associated with different sediment classes, building on recent developments in numerical morphodynamic modeling with heterogeneous sediments (Chavarrías et al., 2019; Stecca et al., 2016; Yager et al., 2007). The observed areal changes in the spatial distribution of wet and dry channel areas cannot be solely attributed to morphological changes brought by the flood. Furthermore, unchanged channel areas may not correspond to the absence of morphological change at those locations, as a continuous, spatially explicit monitoring of the changes in bed elevation during the flood is not available.

The employed mesohabitat assessment cannot provide information on the habitat suitability that occurs during floods or sediment-transporting events. In fact, the biological models used in nearly all existing habitat modelling approaches are data-driven, repeatable, but obtained at flow conditions that are far from sediment-transporting conditions occurring during floods. Recent research by Rachelly et al. (2021) sheds some light on this aspect. Their laboratory experiments revealed that a reach characterized by equilibrium sediment supply (100% channel transport capacity), probably similar to the downstream subreach, promotes the availability of suitable habitats (called 'refugia' by the authors) during flood events. These conditions can increase lateral connectivity and create shallow, low-flowing areas capable of serving as suitable spaces for fish during such events. This suggests that in the downstream section of the Spöl, the flood event may have formed areas where fish could seek shelter from the high flow velocities characteristic of the flood. Furthermore, during floods, certain HMUs (e.g., deep pools with enduring structures) may provide refugia from the flushing flows (Harvey et al., 1999; Schwartz & Herricks, 2005; Tschaplinski & Hartman, 1983). From a habitat perspective, the ecological function of some of these HMUs will change with different discharges, where a pool with almost stagnant water at low flow conditions can transition into a deep run with high velocity, water depth and shear stress at high flows (Wegscheider et al.2020).

The work has compared the HMU mosaics before and after one experimental flood at comparable low flow conditions but cannot provide information on how these mosaics differ over a broader range of flow conditions. It was not designed to compare the so-called 'habitat-streamflow rating curves' between the two reaches and their possible change because of the flood. This would be of high management interest and should be analyzed in future work.

Finally, the choice of representative subreaches for mesohabsim surveys within longer homogeneous reaches does not explicitly account for several elements that might play an important role in habitat suitability, especially when considering a range of different flow conditions, like the spatial distribution of driftwood. This matter deserves further investigation.

6 | CONCLUSIONS

Experimental floods are often aimed at improving and restoring the ecological conditions of rivers. In this research, we studied the morphological and fish habitat dynamics linked to an experimental flood under different sediment availability but similar flow conditions during the flood. The analysis integrated geomorphological observations, analytical morphodynamic theories, hydraulic and sediment measurements and habitat modelling and was structured into a reach-scale and mesoscale analysis of morphological and habitat dynamics. The designed ecological flood was unable to drive relevant morphological and habitat change in the upstream reach. Downstream the confluence, the large amounts of sediment supply over time resulted in a much more dynamic river reach. A key finding is the absence of a direct correlation between changes in morphology and mesoscale habitat suitability. For example, the 45% change in morphology caused by the flood in the downstream reach only resulted in minor changes in terms of habitat suitability for both adult (+10%) and juvenile (+1%) brown trout. The paucity of in-stream structures observed across the lower Spöl motivates the relatively low predicted habitat suitabilities, suggesting that their presence could significantly improve it. Differences in the observed morphological changes can be attributed to two main factors: (i) the prolonged bedload mobility conditions and (ii) the occurrence of bar migration, which were more pronounced in the downstream reach compared to the upstream one. Our work supports the relevance of integrating morphodynamic modelling with geomorphological and eco-hydraulic analysis when planning experimental floods and confirms the importance of carefully considering the role of sediment supply from lateral tributaries downstream of the dam.

AUTHOR CONTRIBUTIONS

Tulio Soto Parra: Conceptualisation; methodology; data curation; formal analysis, visualization; writing—original draft. **Emilio Politti:** Methodology; resources. **Guido Zolezzi:** Conceptualisation; funding acquisition; methodology; writing—review and editing.

ACKNOWLEDGEMENTS

This research is funded by the European Union's Horizon 2020 Research and Innovation Programme under MSCA grant no. 765553 within the EuroFLOW project. We extend our appreciation to our dedicated colleagues who actively participated in the 2021 field campaign. We are grateful to the Swiss National Park Research team for their invaluable assistance and support in providing crucial data for our research endeavours. G. Zolezzi acknowledges the Italian Ministry of Universities and Research (MUR) in the framework of the project DICAM-EXC (Department of Excellence 2023–2027, grant L232/2016). We acknowledge the support of the MUR PNRR project INEST- Interconnected Nord-Est Innovation Ecosystem (ECS00000043) funded by the NextGenerationEU. Open access publishing facilitated by Universita degli Studi di Trento, as part of the Wiley - CRUI-CARE agreement.

CONFLICT OF INTEREST STATEMENT

The authors declare no potential conflicts of interest.

DATA AVAILABILITY STATEMENT

Data for this study are available from the authors on request.

PERMISSION TO REPRODUCE MATERIAL FROM OTHER SOURCES

The manuscript does not include any material reproduced from other sources. All content is original.

ORCID

Tulio Soto Parra https://orcid.org/0009-0003-6320-3091
Guido Zolezzi https://orcid.org/0000-0003-2807-7387

REFERENCES

Acreman, M. (2000) Managed flood releases from reservoirs: issues and guidance prepared for thematic review II. 1: dams, ecosystem functions and environmental restoration go back. Available from: http://www.dams.org/

Adami, L., Bertoldi, W. & Zolezzi, G. (2016) Multidecadal dynamics of alternate bars in the Alpine Rhine river. *Water Resources Research*, 52(11), 8938–8955.

Almeida, G. A. M.D. & Rodróguez, J.F. (2012) Spontaneous formation and degradation of pool-riffle morphology and sediment sorting using a simple fractional transport model. *Geophysical Research Letters*, 39, L06407.

Bathurst, J.C. (1987) Critical conditions for bed material movement in steep, boulder-bed streams. *Erosion and Sedimentation in the Pacific Rim*, 165, 309–318.

Belletti, B., Rinaldi, M., Bussettini, M., Comiti, F., Gurnell, A.M., Mao, L. et al. (2017) Characterising physical habitats and fluvial hydromorphology: a new system for the survey and classification of river geomorphic units. *Geomorphology*, 283, 143–157. Available from: https://www.sciencedirect.com/science/article/pii/S0169555X16305852

Blondeaux, P. & Seminara, G. (1985) A unified bar–bend theory of river meanders. *Journal of Fluid Mechanics*, 157, 449–470.

Boes, R.M., Auel, C., Hagemann, M. & Albayrak, I. (2014) Sediment bypass tunnels to mitigate reservoir sedimentation and restore sediment continuity.

Bovee, K. (1982) A guide to stream habitat analysis using the instream flow incremental methodology. IFIP no. 12.

Bovee, K., Lamb, B.L., Bartholow, J.M., Stalnaker, C.B., Taylor, J. & Henriksen, J. (1998) Stream habitat analysis using the instream flow incremental methodology. U.S. Geological Survey, Available from: https://pubs.er.usgs.gov/publication/itr19980004

Brandt, S.A. (2000) Prediction of downstream geomorphological changes after dam construction: a stream power approach. *International Journal of Water Resources Development*, 16, 343–367.

Brierley, G.J. & Fryirs, K.A. (2013) *Geomorphology and river management: applications of the river styles framework*. John Wiley & Sons.

Bundi, U. (2010) *Alpine waters*, 1 In: Ulrich, B. (Ed.), Vol. 1. Berlin, Heidelberg: Springer. Available from: https://doi.org/10.1007/978-3-540-88275-6

Capra, H., Breil, P. & Souchon, Y. (1995) A new tool to interpret magnitude and duration of fish habitat variations. *Regulated Rivers: Research & Management*, 10(2-4), 281–289.

Chavarrías, V., Stecca, G., Siviglia, A. & Blom, A. (2019) A regularization strategy for modeling mixed-sediment river morphodynamics. *Advances in Water Resources*, 127, 291–309.

Chow, V.T. (1957) Discussion of "integrating the equation of gradually varied flow". *Journal of the Hydraulics Division*, 83(1), 1177–1179.

Chow, V.T. (1959) *Open-channel hydraulics*. McGraw-Hill.

Colombini, M., Seminara, G. & Tubino, M. (1987) Finite-amplitude alternate bars. *Journal of Fluid Mechanics*, 181, 213. Available from: http://www.journals.cambridge.org/abstract_S0022112087002064

Consoli, G., Haller, R.M., Doering, M., Hashemi, S. & Robinson, C.T. (2022) Tributary effects on the ecological responses of a regulated river to experimental floods. *Journal of Environmental Management*, 303, 114122.

Death, R.G. (2008) The effect of floods on aquatic invertebrate communities. In *Aquatic insects: challenges to populations*, CABI; 103–121.

Doering, M., Freimann, R., Antenen, N., Roschi, A., Robinson, C.T., Rezzonico, F. et al. (2021) Microbial communities in floodplain ecosystems in relation to altered flow regimes and experimental flooding. *Science of the Total Environment*, 788, 147497.

Dunbar, M.J., Alfredsen, K. & Harby, A. (2012) Hydraulic-habitat modelling for setting environmental river flow needs for salmonids. *Fisheries Management and Ecology*, 19, 500–517.

Eaton, B.C. & Church, M. (2009) Channel stability in bed load-dominated streams with nonerodible banks: inferences from experiments in a sinuous flume. *Journal of Geophysical Research*, 114, F01024.

Eaton, B.C., MacKenzie, L.G. & Booker, W.H. (2020) Channel stability in steep gravel-cobble streams is controlled by the coarse tail of the bed material distribution. *Earth Surface Processes and Landforms*, 45, 3639–3652. Available from: https://doi.org/10.1002/esp.4994

Ellis, L.E. & Jones, N.E. (2013) Longitudinal trends in regulated rivers: a review and synthesis within the context of the serial discontinuity concept. *Environmental Reviews*, 21, 136–148.

Escobar-Arias, M.I. & Pasternack, G.B. (2010) A hydrogeomorphic dynamics approach to assess in stream ecological functionality using the functional flows model, part 1-model characteristics. *River Research and Applications*, 26, 1103–1128.

European Commission and Directorate-General for Environment (2015) Ecological flows in the implementation of the water framework directive. Guidance document no 31. Publications Office, Available from: http://ec.europa.eu

Fausch, K.D. & White, R.J. (1981) Competition between brook trout (Salvelinus fontinalis) and brown trout (Salmo trutta) for positions in a michigan stream.

Ferrer-Boix, C. & Hassan, M.A. (2014) Influence of the sediment supply texture on morphological adjustments in gravel-bed rivers. *Water Resources Research*, 50, 8868–8890.

Fryirs, K.A. (2017) River sensitivity: a lost foundation concept in fluvial geomorphology. *Earth Surface Processes and Landforms*, 42, 55–70.

Graf, W.L. (2006) Downstream hydrologic and geomorphic effects of large dams on american rivers. *Geomorphology*, 79, 336–360.

Greig, S., Sear, D. & Carling, P. (2007) A field-based assessment of oxygen supply to incubating Atlantic salmon (Salmo salar) embryos. *Hydrological Processes*, 21, 3087–3100.

Gurnell, A.M., Rinaldi, M., Belletti, B., Bizzi, S., Blamauer, B., Braca, G. et al. (2016) A multi-scale hierarchical framework for developing understanding of river behaviour to support river management. *Aquatic*

Sciences, 78, 1–16. Available from: http://link.springer.com/10.1007/s00027-015-0424-5

Harvey, B.C., Nakamoto, R.J. & White, J.L. (1999) Influence of large woody debris and a bankfull flood on movement of adult resident coastal cutthroat trout (Oncorhynchus clarki) during fall and winter.

Hashemi, S., Carrivick, J. & Klaar, M. (2023) Hydromorphological response of heavily modified rivers to flood releases from reservoirs: a case study of the Spöl River, Switzerland. *Earth Surface Processes and Landforms*, 49, 1028–1046. Available from: https://onlinelibrary.wiley.com/doi/10.1002/esp.5749

Herschy, R. (1993) The velocity-area method. *Flow Measurement and Instrumentation*, 4, 7–10.

Ingendahl, D. (2001) Dissolved oxygen concentration and emergence of sea trout fry from natural redds in tributaries of the River Rhine. *Journal of Fish Biology*, 58, 325–341.

Jalón, D. G.D., Bussettini, M., Rinaldi, M., Grant, G., Friberg, N., Cowx, I.G. et al. (2017) Linking environmental flows to sediment dynamics. *Water Policy*, 19, 358–375.

Kemp, J.L., Harper, D.M., Crosa, G.A. & Kemp, J.L. (1999) Use of 'functional habitats' to link ecology with morphology and hydrology in river rehabilitation.

Kennard, M.J., Pusey, B.J., Olden, J.D., MacKay, S.J., Stein, J.L. & Marsh, N. (2010) Classification of natural flow regimes in Australia to support environmental flow management. *Freshwater Biology*, 55, 171–193.

King, J. & Louw, D. (1998) Instream flow assessments for regulated rivers in South Africa using the building block methodology. *Aquatic Ecosystem Health and Management*, 1, 109–124.

Lamb, M.P., Dietrich, W.E. & Venditti, J.G. (2008) Is the critical shields stress for incipient sediment motion dependent on channel-bed slope?. *Journal of Geophysical Research: Earth Surface*, 113, F02008.

Lane, S., Gaillet, T. & Goldenschue, L. (2022) Restoring morphodynamics downstream from alpine dams: development of a geomorphological version of the serial discontinuity concept. *Geomorphology*, 402, 108131. Available from: https://www.sciencedirect.com/science/article/pii/S0169555X22000241

Lane, S., Gentile, A. & Goldenschue, L. (2020) Combining UAV-based SFM-MVS photogrammetry with conventional monitoring to set environmental flows: modifying dam flushing flows to improve alpine stream habitat. *Remote Sensing*, 12, 1–35.

Mannes, S., Robinson, C.-T., Uehlinger, U., Scheurer, T., Ortlepp, J., Mürle, U. et al. (2008) Ecological effects of a long-term flood program in a flow-regulated river. *Revue de Géographie Alpine* 96-1: 125–134.

Mathers, K.L., Robinson, C.T. & Weber, C. (2021) Artificial flood reduces fine sediment clogging enhancing hyporheic zone physicochemistry and accessibility for macroinvertebrates. *Ecological Solutions and Evidence*, 2, e12103. Available from: https://doi.org/10.1002/2688-8319.12103

Mathers, K.L., Robinson, C.T. & Weber, C. (2022) Patchiness in flow refugia use by macroinvertebrates following an artificial flood pulse. *River Research and Applications*, 38, 696–707. Available from: https://doi.org/10.1002/rra.3941

Meyer-Peter, E. & Müller, R. (1948) Formulas for bed-load transport, Iahsr 2nd Meeting, Stockholm, Appendix 2, IAHR.

Miwa, H. & Nagayoshi, T. (1999) Suppression limit of alternate bar migration through sine-generated meander channels. *Journal of Natural Disaster Science*, 21(1), 1–10.

Montgomery, D.R. & Buffington, J.M. (1997) Channel-reach morphology in mountain drainage basins. *Bulletin of the Geological Society of America*, 109, 596–611.

Mueller, E.R. & Pitlick, J. (2013) Sediment supply and channel morphology in mountain river systems: 1. Relative importance of lithology, topography, and climate. *Journal of Geophysical Research: Earth Surface*, 118, 2325–2342.

Nelson, J.M. (1990) The initial instability and finite-amplitude stability of alternate bars in straight channels. *Earth-Science Reviews*, 29(1-4), 97–115.

Ortlepp, J. & Mürle, U. (2003) Effects of experimental flooding on brown trout (Salmo trutta fario l.): the River Spöl, Swiss National Park. *Aquatic Sciences*, 65, 232–238.

Parasiewicz, P. (2007) The MesoHABSIM model revisited. *River Research and Applications*, 23, 893–903.

Parasiewicz, P. (2014) The MesoHABSIM) model revisited. *River Research and Applications*, 30, 132–133.

Parker, G. (1990) Surface-based bedload transport relation for gravel rivers. *Journal of Hydraulic Research*, 28, 417–436.

Pellegrini, G., Martini, L., Rainato, R. & Picco, L. (2022) Large wood mobilization and morphological changes in an alpine river following the release of an ordinary experimental flood from an upstream dam. *CATENA*, 216, 106398.

Poff, N.L. (2002) Ecological response to and management of increased flooding caused by climate change. *Philosophical Transactions of the Royal Society of London. Series A: Mathematical, Physical and Engineering Sciences*, 360, 1497–1510.

Poff, N.L., Allan, J.D., Bain, M.B., Karr, J.R., Prestegaard, K.L., Richter, B.D. et al. (1997) The natural flow regime. *BioScience*, 47, 769–784. Available from: https://academic.oup.com/bioscience/article-lookup/doi/10.2307/1313099

Poff, N.L. & Matthews, J.H. (2013) Environmental flows in the anthropocence: past progress and future prospects. *Current Opinion in Environmental Sustainability*, 5, 667–675.

Polzin, M. & Rood, S. (2006) Effective disturbance: seedling safe sites and patch recruitment of riparian cottonwoods after a major flood of a mountain river. *Wetlands*, 26, 965–980.

Rachelly, C., Mathers, K.L., Weber, C., Weitbrecht, V., Boes, R.M. & Vetsch, D.F. (2021) How does sediment supply influence refugia availability in river widenings?. *Journal of Ecohydraulics*, 6, 121–138. Available from: https://www.tandfonline.com/doi/full/10.1080/24705357.2020.1831415

Rachelly, C., Vetsch, D.F., Boes, R.M. & Weitbrecht, V. (2022) Sediment supply control on morphodynamic processes in gravel-bed river widenings. *Earth Surface Processes and Landforms*, 47, 3415–3434. Available from: https://onlinelibrary.wiley.com/doi/10.1002/esp.5460

Richter, B.D., Baumgartner, J.V., Powell, J. & Braun, D.P. (1996) A method for assessing hydrologic alteration within ecosystems. *Conservation Biology*, 10(4), 11634174.

Rinaldi, M., Surian, N., Comiti, F. & Bussettini, M. (2013) A method for the assessment and analysis of the hydromorphological condition of Italian streams: the morphological quality index (mqi). *Geomorphology* 180-181: 96–108. Available from: https://linkinghub.elsevier.com/retrieve/pii/S0169555X12004461

Robinson, C.T., Consoli, G. & Ortlepp, J. (2023) Importance of artificial high flows in maintaining the ecological integrity of a regulated river. *Science of The Total Environment*, 882, 163569. Available from: https://linkinghub.elsevier.com/retrieve/pii/S0048969723021885

Robinson, C.T., Molinari, P., Mürle, U., Ortlepp, J., Scheurer, T., Uehlinger, U. et al. (2017) Experimental floods to improve the integrity of regulated rivers. *GAIA - Ecological Perspectives for Science and Society*, 13, 186–190.

Robinson, C.T., Siebers, A.R. & Ortlepp, J. (2018) Long-term ecological responses of the River Spöl to experimental floods. *Freshwater Science*, 37, 433–447.

Robinson, C.T., Uehlinger, U. & Monaghan, M.T. (2003) Effects of a multi-year experimental flood regime on macroinvertebrates downstream of a reservoir. *Aquatic Sciences*, 65, 210–222.

Robison, E.G. & Beschta, R.L. (1990) Characteristics of coarse woody debris for several coastal streams of Southeast Alaska, USA. Available from: www.nrcresearchpress.com

Ruiz-Villanueva, V., Aarnink, J., Gibaja, J., Finch, B. & Vuaridel, M. (2022) Integrating flow-, sediment- and wood-regimes during e-flows in the Spöl River (Swiss Alps), International Association for Hydro-Environment Engineering and Research (IAHR).

Scheurer, T. & Molinari, P. (2003) Experimental floods in the River Spöl, Swiss National Park: framework, objectives and design. *Aquatic Sciences*, 65, 183–190.

Schneider, M., Noack, M., Gebler, T. & Kopecki, L. (2010) Handbook for the habitat simulation model Casimir. Module Casimir-fish. Base version. SJE–Schneider & Jorde Ecological Engineering GmbH. LWW–Institut fur Wasserbau, Universitat Stuttgart.

Schumm, S.A. (1977) The fluvial system.

Schwartz, J.S. & Herricks, E.E. (2005) Fish use of stage-specific fluvial habitats as refuge patches during a flood in a low-gradient Illinois Stream. *Canadian Journal of Fisheries and Aquatic Sciences*, 62, 1540–1552.

Serlet, A.J., Gurnell, A.M., Zolezzi, G., Wharton, G., Belleudy, P. & Jourdain, C. (2018) Biomorphodynamics of alternate bars in a channelized, regulated river: an integrated historical and modelling analysis. *Earth Surface Processes and Landforms*, 43(9), 1739–1756.

Shields, A. (1936) Anwendung der aehnlichkeitsmechanik und der turbulenzforschung auf die geschiebebewegung. PhD Thesis, Technical University Berlin.

Sommer, T.R., Nobriga, M.L., Harrell, W.C., Batham, W. & Kimmerer, W.J. (2001) Floodplain rearing of juvenile Chinook salmon: evidence of enhanced growth and survival. *Canadian Journal of Fisheries and Aquatic Sciences*, 58, 325–333. Available from: http://www.nrcresearchpress.com/doi/10.1139/f00-245

Stecca, G., Siviglia, A. & Blom, A. (2016) An accurate numerical solution to the Saint-Venant-Hirano model for mixed-sediment morphodynamics in rivers. *Advances in Water Resources*, 93, 39–61.

Surian, N. (1999) Channel changes due to river regulation: the case of the Piave River, Italy. *Earth Surface Processes and Landforms*, 24, 1135–1151.

Surian, N. & Cisotto, A. (2007) Channel adjustments and bedload transport in the Brenta river 1641 channel adjustments, bedload transport and sediment sources in a gravel-bed river, Brenta River, Italy. *Earth Surf. Process. Landforms*, 32, 1641–1656. Available from: www.interscience.wiley.com

Suska, K. & Parasiewicz, P. (2020) Application of the mesohabitat simulation system (mesohabsim) for assessing impact of river maintenance and restoration measures. *Water (Switzerland)*, 12, 3356.

Talbot, C.J., Bennett, E.M., Cassell, K., Hanes, D.M., Minor, E.C., Paerl, H. et al. (2018) The impact of flooding on aquatic ecosystem services. *Biogeochemistry*, 141, 439–461.

Terrado, M., Acuña, V., Ennaanay, D., Tallis, H. & Sabater, S. (2014) Impact of climate extremes on hydrological ecosystem services in a heavily humanized mediterranean basin. *Ecological Indicators*, 37, 199–209.

Thorne, C.R., Hey, R.D. & Newson, M.D. (1997) Applied fluvial geomorphology for river engineering and management.

Tschaplinski, P.J. & Hartman, G.F. (1983) Winter distribution of juvenile coho salmon (Oncorhynchus kisutch) before and after logging in Carnation Creek, British Columbia, and some implications for overwinter survival. *Canadian Journal of Fisheries and Aquatic Sciences*, 40(4), 452–461.

van Rooijen, E., Siviglia, A., Vetsch, D.F., Boes, R.M. & Vanzo, D. (2022) Quantifying fluvial habitat changes due to multiple subsequent floods in a braided alpine reach. *Journal of Ecohydraulics*, 9, 1–21. Available from: https://www.tandfonline.com/doi/full/10.1080/24705357.2022.2105755

Vassoney, E., Mochet, A.M., Rocco, R., Maddalena, R., Vezza, P. & Comoglio, C. (2019) Integrating meso-scale habitat modelling in the multicriteria analysis (MCA) process for the assessment of hydropower sustainability. *Water (Switzerland)*, 11, 640.

Vetter, T. (2011) Riffle-pool morphometry and stage-dependant morphodynamics of a large floodplain river (Vereinigte Mulde, Sachsen-Anhalt, Germany). *Earth Surface Processes and Landforms*, 36, 1647–1657.

Vezza, P., Parasiewicz, P., Rosso, M. & Comoglio, C. (2012) Defining minimum environmental flows at regional scale: application of mesoscale habitat models and catchments classification. *River Research and Applications*, 28, 717–730.

Vezza, P., Parasiewicz, P., Spairani, M. & Comoglio, C. (2014) Habitat modeling in high-gradient streams: the mesoscale approach and application. *Ecological Applications*, 24(4), 844–861.

Vezza, P., Zanin, A., Parasiewicz, P. et al. (2017) Manuale tecnico-operativo per la modellazione e la valutazione dell'ntegrità dell' habitat fluviale.

von Freyberg, J., Allen, S.T., Seeger, S., Weiler, M. & Kirchner, J.W. (2018) Sensitivity of young water fractions to hydro-climatic forcing and landscape properties across 22 Swiss catchments. *Hydrology and Earth System Sciences*, 22(7), 3841–3861. Available from: https://hess.copernicus.org/articles/22/3841/2018/

Wegscheider, B., Linnansaari, T. & Curry, R.A. (2020) Mesohabitat modelling in fish ecology: a global synthesis. *Fish and Fisheries*, 21(5), 927–939.

Welber, M., Coz, J.L., Laronne, J.B., Zol (2016) A systematic test of surface velocity radar (SVR) to improve flood discharge prediction h51i-1332. 624.

Whipple, A.A. & Viers, J.H. (2019) Coupling landscapes and river flows to restore highly modified rivers. *Water Resources Research*, 55, 4512–4532.

Wildhaber, Y.S., Michel, C., Epting, J., Wildhaber, R.A., Huber, E., Huggenberger, P. et al. (2014) Effects of river morphology, hydraulic gradients, and sediment deposition on water exchange and oxygen dynamics in Salmonid redds. *Science of The Total Environment* 470-471: 488–500.

Williams, G.P. & Wolman, M.G. (1984) Downstream effects of dams on alluvial rivers.

Wohl, E., Bledsoe, B.P., Jacobson, R.B., Poff, N.L., Rathburn, S.L., Walters, D.M. et al. (2015) The natural sediment regime in rivers: broadening the foundation for ecosystem management. *BioScience*, 65, 358–371.

Wolman, G. (1954) A method of sampling coarse river-bed material. *EOS, Transactions American Geophysical Union*, 35, 951–956. Available from: https://doi.org/10.1029/TR035i006p00951

Yager, E.M., Kirchner, J.W. & Dietrich, W.E. (2007) Calculating bed load transport in steep boulder bed channels. *Water Resources Research*, 43(7), W07418.

Zolezzi, G., Bertoldi, W. & Tubino, M. (2012) Morphodynamics of bars in gravel-bed rivers: bridging analytical models and field observations. In *Gravel-bed rivers: Processes, tools, environments*, Wiley; 69–89.

SUPPORTING INFORMATION

Additional supporting information can be found online in the Supporting Information section at the end of this article.

How to cite this article: Soto Parra, T., Politti, E. & Zolezzi, G. (2024) Morphological and fish mesohabitat dynamics following an experimental flood under different sediment availability. *Earth Surface Processes and Landforms*, 1–19. Available from: https://doi.org/10.1002/esp.6025